

Accepted Manuscript

A Nonlinear Orthogonal Non-Negative Matrix Factorization Approach to Subspace Clustering

Dijana Tolić, Nino Antulov-Fantulin, Ivica Kopriva

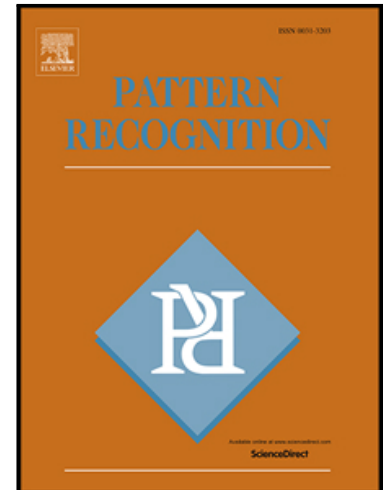
PII: S0031-3203(18)30164-X
DOI: [10.1016/j.patcog.2018.04.029](https://doi.org/10.1016/j.patcog.2018.04.029)
Reference: PR 6543

To appear in: *Pattern Recognition*

Received date: 28 March 2017
Revised date: 22 March 2018
Accepted date: 27 April 2018

Please cite this article as: Dijana Tolić, Nino Antulov-Fantulin, Ivica Kopriva, A Nonlinear Orthogonal Non-Negative Matrix Factorization Approach to Subspace Clustering, *Pattern Recognition* (2018), doi: [10.1016/j.patcog.2018.04.029](https://doi.org/10.1016/j.patcog.2018.04.029)

This is a PDF file of an unedited manuscript that has been accepted for publication. As a service to our customers we are providing this early version of the manuscript. The manuscript will undergo copyediting, typesetting, and review of the resulting proof before it is published in its final form. Please note that during the production process errors may be discovered which could affect the content, and all legal disclaimers that apply to the journal pertain.



Highlights

- Subspace clustering is solved from nonlinear orthogonal NMF perspective.
- General kernel-based multiplicative orthogonal updates for NMF are derived.
- Explicit orthogonality constraint excludes the usual k-means clustering step.
- The local geometric structure is included via fully connected graph regularization.
- A connection between spectral clustering and kernel orthogonal NMF is established.

ACCEPTED MANUSCRIPT

A Nonlinear Orthogonal Non-Negative Matrix Factorization Approach to Subspace Clustering

Dijana Tolić¹

Laboratory for Machine Learning and Knowledge Representations, Ruder Bošković Institute, Zagreb, Croatia, Bijenicka cesta 54, 10000 Zagreb, Croatia

Nino Antulov-Fantulin

ETH Zürich, Swiss Federal Institute of Technology, Clausiusstrasse 50, COSS, CLU, 8092 Zürich, Switzerland

Ivica Kopriva

Laboratory for Machine Learning and Knowledge Representations, Ruder Bošković Institute, Zagreb, Croatia, Bijenicka cesta 54, 10000 Zagreb, Croatia

Abstract

A recent theoretical analysis shows the equivalence between non-negative matrix factorization (NMF) and spectral clustering based approach to subspace clustering. As NMF and many of its variants are essentially linear, we introduce a nonlinear NMF with explicit orthogonality and derive general kernel-based orthogonal multiplicative update rules to solve the subspace clustering problem. In nonlinear orthogonal NMF framework, we propose two subspace clustering algorithms, named kernel-based non-negative subspace clustering KNSC-Ncut and KNSC-Rcut and establish their connection with spectral normalized cut and ratio cut clustering. We further extend the nonlinear orthogonal NMF framework and introduce a graph regularization to obtain a factorization that respects a local geometric structure of the data after the nonlinear mapping. The proposed NMF-based approach to subspace clustering takes into account the nonlinear nature of the manifold, as well as its intrinsic local geometry, which considerably improves the clustering performance when compared to the several recently proposed state-of-the-art methods.

Keywords: subspace clustering, non-negative matrix factorization, orthogonality, kernels, graph regularization

1 Introduced in [1] as a parts-based low-rank representation of the original data matrix, non-negative
 2 matrix factorization (NMF) has shown to be a useful decomposition of multivariate data [2, 3, 4]. The
 3 most important feature of NMF is the non-negativity of all elements of the matrices involved, which
 4 allows an additive parts-based decomposition of the data. This non-negativity is often encountered in
 5 real world data, providing a natural interpretation in contrast to other decomposition techniques that

¹Corresponding author - email: dijana.tolic@irb.hr, tel: +385 1 457 1352

6 allow negative combinations (such as SVD). Related NMF factorizations include convex NMF, orthogonal
7 NMF and kernel NMF [5, 6, 7, 8, 9, 10].

8 The key idea in subspace clustering is to construct a weighted affinity graph from the initial data set,
9 such that each node represents a data point and each weighted edge represents the similarity based on
10 distance between each pair of points (e.g. the Euclidean distance). Spectral clustering then finds the
11 cluster membership of the data points by using the spectrum of an affinity graph.

12 State-of-the-art methods in single view subspace clustering learn affinity graph matrix by imposing
13 sparseness [11], low-rank [12] or jointly sparseness and low-rank constraints [13] on representation matrix.
14 In multi-view subspace clustering representation matrices across views can be learnt by utilization of in-
15 dependence criterion which decreases redundancy between representations [14]. Joint low-rank sparseness
16 constrained approach can be extended to multi-view clustering [15]. The NMF methods proposed herein
17 to handle single view subspace clustering problem can be extended to NMF-based multi-view subspace
18 clustering [16]. Furthermore, the methods proposed by us could possibly improve performance further
19 through post-processing step that re-assigns samples to more suitable clusters [17].

20 Spectral clustering can be seen as a graph partition problem and solved by the eigenvalue decom-
21 position of the graph Laplacian matrix [18, 19, 20, 21, 22]. In particular, there is a close relationship
22 between the eigenvector corresponding to the second eigenvalue of the Laplacian and the graph cut
23 problem [23, 24]. However, the complexity of optimizing graph cut objective function is high, e.g. the
24 optimization of the normalized cut (Ncut) is known to be an NP-hard problem [5, 25, 26, 27]. Spectral
25 clustering seeks to get the relaxed solution, which is an approximate solution for the graph partition.
26 Compared with conventional clustering algorithms, spectral clustering has advantages to converge to
27 global optimum and performs well for the sample space of arbitrary shape [26, 18, 19, 28].

28 Despite empirical success of spectral clustering, one drawback is that a mixed-signed result given
29 by the eigenvalue decomposition of the Laplacian may lack clustering interpretability or degrade the
30 clustering performance [2]. The computational complexity of the eigenvalue decomposition is $\mathcal{O}(n^3)$,
31 where n denotes the number of points. To avoid the computation of eigenvalues and eigenvectors, a
32 recently established connection of the spectral clustering and non-negative matrix factorization (NMF)
33 was utilized in [29, 30] and [31]. As pointed out in [30], the formulation of non-negative spectral clustering
34 is motivated by practical reasons: (i) one can use the update algorithms of NMF to solve spectral
35 clustering, and (ii) NMF framework can easily incorporate additional constraints to spectral clustering
36 algorithms.

37 It was shown in [30] that spectral clustering Ncut can be treated as a symmetric NMF problem of
38 the graph affinity matrix constructed from the data matrix. Similarly, it was also proven that the Rcut
39 spectral clustering is equivalent to the symmetric NMF of the graph affinity matrix, introducing the
40 non-negative Laplacian embedding (NLE) [31]. Both results [30, 31] only factorize the graph affinity

41 matrix, imposing the assumption that the input data comes in as a matrix of pairwise similarities. The
 42 factorization of the graph affinity matrix was replaced with the factorization of the data matrix itself
 43 in [29], and including an additional global discriminative regularization term in [32]. However, both
 44 NMF-based NSC methods [29, 32], minimize data fidelity term in the linear input space.

45 In this paper we propose a nonlinear orthogonal NMF approach to subspace clustering. We estab-
 46 lish an equivalence with spectral clustering and propose two non-negative spectral clustering algorithms,
 47 named *kernel-based non-negative spectral clustering* KNSC-Ncut and KNSC-Rcut. To further explore the
 48 nonlinear orthogonal NMF framework, we also introduce a graph regularization term [4] which captures
 49 the intrinsic local geometric structure in the nonlinear feature space. By preserving the geometric struc-
 50 ture, the graph regularization term allows the factorization method to have more discriminating power
 51 for clustering data points sampled from a submanifold which lies in a higher dimensional ambient space
 52 [4].

53 Recently, a similar connection between kernel PCA and spectral methods has been shown in [33, 18,
 54 28, 34]. Our method gives an insight into the connection between kernel NMF and spectral methods,
 55 where the kernel matrix from multiplicative updates corresponds to the nonlinear graph affinity matrix
 56 in spectral clustering. Different from [29, 32, 30, 31], our equivalence is established by directly factorizing
 57 the nonlinearity mapped input data matrix. To the best of our knowledge, this is the first approach to
 58 non-negative spectral clustering that uses kernel orthogonal NMF.

59 By constraining the orthogonality of the clustering matrix during the nonlinear NMF updates, the
 60 cluster membership can be obtained directly from the orthogonal clustering matrix, avoiding the need
 61 of usual k -means clustering [29, 30, 31, 32]. The proposed approach has a total run-time complexity of
 62 $\mathcal{O}(kn^2)$ for clustering n data points to k clusters, which is less than standard spectral clustering methods
 63 $\mathcal{O}(n^3)$ and the same complexity as the state-of-the-art methods [29, 32, 35].

64 We perform a comprehensive analysis of our approach, including the convergence proofs for the kernel-
 65 based graph regularized orthogonal multiplicative update rules. We conduct extensive experiments to
 66 compare our methods with other non-negative spectral clustering methods and further perform the sen-
 67 sitivity analysis of the parameters used in our approach. We highlight here the main contributions of the
 68 paper:

- 69 1. We formulate a nonlinear NMF with explicitly enforced orthogonality to address the subspace
 70 clustering problem.
- 71 2. We derive kernel-based orthogonal multiplicative updates to solve the constrained non-convex
 72 nonlinear NMF problem. We perform the convergence analysis for the multiplicative updates and give
 73 the convergence proofs using an auxiliary function approach [36].
- 74 3. We formulate a nonlinear (kernel-based) orthogonal graph regularized NMF approach to subspace
 75 clustering. The ability of the proposed method to exploit both the nonlinear nature of the manifold as

76 well as its local geometric structure considerably improves the clustering performance.

77 4. The proposed clustering algorithms provide an insight into the connection between the spectral
78 clustering methods and kernel NMF, where the kernel matrix in the kernel-based NMF multiplicative
79 updates corresponds to the nonlinear graph affinity matrix in Ncut and Rcut spectral clustering.

80 The rest of the paper is organized as follows: in Section 1 we present a brief overview of the NMF-
81 based spectral clustering. In Section 2, we propose our framework and present three non-negative spectral
82 clustering algorithms, along with the theoretical results on the equivalence of our approach and non-
83 negative spectral clustering. In Section 3, we compare our methods to the 9 recently proposed non-
84 negative spectral clustering methods on 6 data sets. Lastly, we give the conclusions in Section 4.

85 1. Related work

86 We denote all matrices with bold upper case letters, all vectors with bold lower case letters. \mathbf{A}^\top
87 denotes the transpose of the matrix \mathbf{A} , and \mathbf{A}^{-1} denotes the inverse of the matrix \mathbf{A} . \mathbf{I} denotes the
88 identity matrix. The Frobenius norm is denoted as $\|\cdot\|_F$. The trace of the matrix is denoted with $\text{Tr}(\cdot)$.
89 In Table 1 we summarize the rest of the notation.

Table 1: *Notations*

Notation	Definition
m	the dimensionality of a data set
n	the number of data points
k	the number of clusters
\mathcal{L}	the Lagrangian
$\mathbf{K} \in \mathbb{R}^{n \times n}$	the kernel matrix
$\mathbf{X} \in \mathbb{R}^{m \times n}$	the input data matrix
$\mathbf{A} \in \mathbb{R}^{n \times n}$	the graph affinity matrix
$\mathbf{D} \in \mathbb{R}^{n \times n}$	the degree matrix based on \mathbf{A}
$\mathbf{L} \in \mathbb{R}^{n \times n}$	the graph Laplacian
$\mathbf{L}_{sym} \in \mathbb{R}^{n \times n}$	the normalized graph Laplacian
$\Phi(\mathbf{X}) \in \mathbb{R}^{D \times n}$	the nonlinear mapping
$\mathbf{H}, \mathbf{Z} \in \mathbb{R}^{k \times n}$	the cluster indicator matrices
$\mathbf{V} \in \mathbb{R}^{m \times k}$	the basis matrix in input space
$\mathbf{F} \in \mathbb{R}^{n \times k}$	the basis matrix in mapped space

90 1.1. Definitions

The task of subspace clustering is to find a low-dimensional subspace to fit each group of data points [37, 38, 39, 40]. Let $\mathbf{X} \in \mathbb{R}^{m \times n}$ denote the data matrix $m \times n$ which is comprised of n data points $\mathbf{x}_i \in \mathbb{R}^m$, drawn from a union of k linear subspaces $S_1 \cup S_2 \cup \dots \cup S_k$ of dimensions $\{m_i\}_{i=1}^k$. Let $X_i \in \mathbb{R}^{m \times n_i}$ be a submatrix of \mathbf{X} of rank m_i with $\sum_{i=1}^k n_i = n$. Given the input matrix \mathbf{X} , subspace clustering assigns data

points according to their subspaces. The first step is to construct a weighted similarity graph $G(V, E)$ from \mathbf{X} , such that each node from the node set $V = \{1, 2, \dots, n\}$ represents a data point $\mathbf{x}_i \in \mathbb{R}^m$ and each weighted edge represents a similarity based on distance (*e.g.* the Euclidean distance) between the corresponding pair of nodes. Typical methods to construct the similarity graph are ϵ -neighbourhood graphs, k -nearest neighbour graphs and fully connected graphs with Gaussian similarity function [4, 41]. Spectral clustering then finds the cluster membership of data points by using the spectrum of the graph Laplacian matrix. Let $\mathbf{A} \in \mathbb{R}^{n \times n}$ be a symmetric affinity matrix of the graph and $A_{ij} \geq 0$ be the pairwise similarity between the nodes. The degree matrix \mathbf{D} based on \mathbf{A} is defined as the diagonal matrix with the degrees d_1, \dots, d_n on the diagonal, where the degree d_i of a node i is

$$d_i = \sum_{j=1}^n A_{ij} \quad (1)$$

Given a weighted graph $G(V, E)$ its unnormalized graph Laplacian matrix \mathbf{L} is given as [42]

$$\mathbf{L} = \mathbf{D} - \mathbf{A} \quad (2)$$

The symmetric normalized graph Laplacian matrix \mathbf{L}_{sym} is defined as

$$\mathbf{L}_{sym} = \mathbf{D}^{-1/2} \mathbf{L} \mathbf{D}^{-1/2} = \mathbf{I} - \mathbf{D}^{-1/2} \mathbf{A} \mathbf{D}^{-1/2} \quad (3)$$

91 where \mathbf{I} is the identity matrix.

92 1.2. Graph cuts

The spectral clustering can be seen as partitioning a similarity graph $G(V, E)$ into a set of nodes $S \subset V$ separated from the complementary set $\bar{S} = V \setminus S$. Depending on the choice of the function to optimize, the graph partition problem can be defined in different ways. The simplest choice of the function is the *cut* $s(S, \bar{S})$ defined as $s(S, \bar{S}) = \sum_{v_i \in S, v_j \in \bar{S}} A_{ij}$. To achieve a better balance in the cardinality of S and \bar{S} , the Ncut and Rcut optimization functions are proposed [42, 43, 44]. Let \mathbf{h}_l be the indicator vector for cluster C_l , i.e. $\mathbf{h}_l(i) = 1$ if $\mathbf{x}_i \in C_l$, otherwise $\mathbf{h}_l(i) = 0$, then $|C_l| = \mathbf{h}_l \mathbf{h}_l^\top$. The cluster indicator matrix $\mathbf{H} \in \mathbb{R}^{k \times n}$ can be defined as

$$\mathbf{H}^\top = \left(\frac{\mathbf{h}_1}{\|\mathbf{h}_1\|}, \frac{\mathbf{h}_2}{\|\mathbf{h}_2\|}, \dots, \frac{\mathbf{h}_k}{\|\mathbf{h}_k\|} \right) \quad (4)$$

Evidently, $\mathbf{H} \mathbf{H}^\top = \mathbf{I}$. Rcut spectral clustering can be formulated as the following optimization problem

$$\min_{\mathbf{H}} \text{Tr}(\mathbf{H} \mathbf{L} \mathbf{H}^\top) \quad s.t. \quad \mathbf{H} \mathbf{H}^\top = \mathbf{I} \quad (5)$$

where $\text{Tr}(\cdot)$ denotes the trace of a matrix and \mathbf{L} is the graph Laplacian. Similarly, define the cluster indicator vector as $\mathbf{z}_k = \mathbf{D}^{1/2} \mathbf{h}_k / \|\mathbf{D}^{1/2} \mathbf{h}_k\|$ and the cluster indicator matrix as $\mathbf{Z}^\top = (\mathbf{z}_1, \mathbf{z}_2, \dots, \mathbf{z}_k)$ where $\mathbf{Z} \in \mathbb{R}^{k \times n}$. Then Ncut is formulated as the minimization problem

$$\min_{\mathbf{Z}} \text{Tr}(\mathbf{Z} \mathbf{L}_{sym} \mathbf{Z}^\top) \quad s.t. \quad \mathbf{Z} \mathbf{Z}^\top = \mathbf{I} \quad (6)$$

93 By allowing the cluster indicator matrices (\mathbf{H} , \mathbf{Z}) to be continuous valued the problem is solved by
 94 eigenvalue decomposition of the graph Laplacian matrix given in Eqs. (2) and (3) [18, 19, 28].

95 1.3. NMF approach to non-negative spectral clustering

The connection between the Ncut spectral clustering and symmetric NMF has been established in [30]

$$\mathbf{D}^{-1/2} \mathbf{A} \mathbf{D}^{-1/2} = \mathbf{H}^T \mathbf{H}, \quad s.t. \quad \mathbf{H} \geq 0. \quad (7)$$

According to the Theorem 2 from [30], enforcing symmetric factorization approximately retains the orthogonality of \mathbf{H} . Similarly, according to the Theorem 5 from [31] the Rcut spectral clustering has been proved to be equivalent to the following symmetric NMF problem

$$\mathbf{A} - \mathbf{D} + \sigma \mathbf{I} = \mathbf{H}^T \mathbf{H}, \quad s.t. \quad \mathbf{H} \mathbf{H}^T = \mathbf{I}, \quad \mathbf{H} \geq 0 \quad (8)$$

where σ is the largest eigenvalue of the graph Laplacian matrix \mathbf{L} and the matrix $\mathbf{H} \in \mathbb{R}^{k \times n}$ contains cluster membership information that data point \mathbf{x}_i belongs to the cluster c_i

$$c_i = \operatorname{argmax}_{1 \leq j \leq k} \mathbf{H}_{ji}. \quad (9)$$

96 In Eqs. (7) and (8) a factorization of $n \times n$ symmetric similarity matrix \mathbf{A} has a complexity $\mathcal{O}(kn^2)$ for
 97 k clusters.

Based on the results [30, 31], in [29] it is proved that for non-negative input data matrix \mathbf{X} , and fully connected graph affinity matrix \mathbf{A} given as the standard inner product $\mathbf{A} = \mathbf{X}^T \mathbf{X}$, Ncut spectral clustering is equivalent to the NMF of the scaled input data matrix (NSC-Ncut)

$$\mathbf{D}^{-1/2} \mathbf{X}^T \approx \mathbf{Z}^T \mathbf{Y} \quad s.t. \quad \mathbf{Z} \mathbf{Z}^T = \mathbf{I}, \mathbf{Z} \geq 0 \quad (10)$$

with cluster indicator matrix $\mathbf{Z} \in \mathbb{R}^{k \times n}$. Similarly, the Theorem 2 [29] establishes the connection of Rcut non-negative spectral clustering (NSC-Rcut) and NMF problem

$$\mathbf{X}^T \approx \mathbf{H}^T \mathbf{Y} \quad s.t. \quad \mathbf{H} \mathbf{H}^T = \mathbf{I}, \mathbf{H} \geq 0 \quad (11)$$

98 with cluster indicator matrix $\mathbf{H} \in \mathbb{R}^{k \times n}$. Both NMF-based approaches to non-negative spectral clustering
 99 (10) and (11) are formulated in the input data space as a factorization of an input data matrix $\mathbf{X} \in \mathbb{R}^{m \times n}$
 100 with the complexity $\mathcal{O}(nmk)$ [29]. The matrix factorization in Eqs. (10) and (11) is limited to the graph
 101 affinity matrix defined as an inner product of the input data matrix.

102 Furthermore, the global discriminative NMF-based NSC model introduced in [32], includes an addi-
 103 tional nonlinear discriminative regularization term to the NMF optimization function proposed in [29].
 104 As shown in [32], the global discriminant information greatly improves the accuracy of NSC-Ncut and
 105 NSC-Rcut [29]. Although in [32] the nonlinear character of the manifold is taken into account through
 106 the nonlinear discriminative matrix, the NMF data fidelity terms are still defined in the input data space.

107 2. Nonlinear orthogonal NMF approach to subspace clustering

108 In this section we develop a nonlinear orthogonal NMF approach to subspace clustering and establish
 109 its equivalence with Ncut and Rcut spectral clustering algorithms. We generalize the NMF objective
 110 function to a nonlinear transformation of the input data and derive kernel-based NMF update rules with
 111 explicitly imposed orthogonality constraints on the clustering matrix \mathbf{H} (or \mathbf{Z}). Enforcing the explicit
 112 orthogonality into the multiplicative rules allows obtaining the cluster membership directly from the
 113 cluster indicator matrix. In this way, we obtain a formulation of the nonlinear NMF that explicitly
 114 addresses the subspace clustering problem.

115 2.1. Kernel-based orthogonal NMF multiplicative updates

116 In this paper we emphasize the orthogonality of the nonlinear NMF to keep the clustering interpre-
 117 tation while taking into account the nonlinearity of the space data are drawn from. We enforce rigorous
 118 orthogonality constraint into the NMF optimization problem and seek to obtain kernel-based orthogonal
 119 multiplicative update rules to solve it.

Let $\mathbf{X} = (\mathbf{x}_1, \mathbf{x}_2, \dots, \mathbf{x}_n) \in \mathbb{R}^{m \times n}$ be the data matrix of non-negative elements. The NMF factorizes \mathbf{X} into two low-rank non-negative matrices

$$\mathbf{X} \approx \mathbf{V}\mathbf{H} \quad (12)$$

where $\mathbf{V} = (\mathbf{v}_1, \mathbf{v}_2, \dots, \mathbf{v}_k) \in \mathbb{R}^{m \times k}$ and $\mathbf{H}^\top = (\mathbf{h}_1, \mathbf{h}_2, \dots, \mathbf{h}_k) \in \mathbb{R}^{n \times k}$ and k is a prespecified rank parameter. Generally, the rank of matrices \mathbf{V} and \mathbf{H} is much lower than the rank of \mathbf{X} (i.e., $k \ll \min(m, n)$). The non-negative matrices \mathbf{V} and \mathbf{H} are obtained by solving the following minimization problem

$$\min_{\mathbf{V}, \mathbf{H} \geq 0} \|\mathbf{X} - \mathbf{V}\mathbf{H}\|_F^2 \quad (13)$$

Consider now a nonlinear transformation (a mapping) to the higher D -dimensional (or infinite) space $\mathbf{x}_i \rightarrow \Phi(\mathbf{x}_i)$ or $\mathbf{X} \rightarrow \Phi(\mathbf{X}) = (\Phi(\mathbf{x}_1), \Phi(\mathbf{x}_2), \dots, \Phi(\mathbf{x}_n)) \in \mathbb{R}^{D \times n}$. The nonlinear NMF problem aims to find two non-negative matrices \mathbf{W} and \mathbf{H} whose product can approximate the mapping of the original matrix $\Phi(\mathbf{X})$

$$\Phi(\mathbf{X}) \approx \mathbf{W}\mathbf{H} \quad (14)$$

For instance, we can consider nonlinear data set composed of two rings as in Fig. 1. The standard linear NMF (13) [45] is not able to separate the two nonlinear clusters. Compared with the solution of Eq. (17), the nonlinear NMF is able to produce the nonlinear separating hypersurfaces between the clusters. We formulate the objective function for the nonlinear orthogonal NMF as

$$\min_{\mathbf{H}, \mathbf{F} \geq 0} \|\Phi(\mathbf{X}) - \mathbf{W}\mathbf{H}\|_F^2 \quad s.t. \quad \mathbf{H}\mathbf{H}^\top = \mathbf{I} \quad (15)$$

Here, \mathbf{W} is the basis in feature space and \mathbf{H} is the clustering matrix. It is worth noting that since Φ can be infinite dimensional, it is impossible to directly factorize $\Phi(\mathbf{X})$ [22, 21, 7]. In what follows we

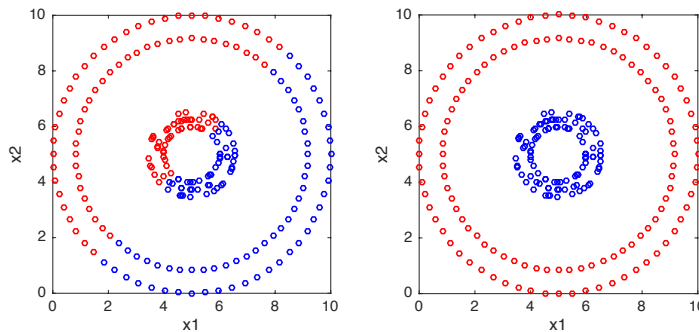


Figure 1: Clustering with NMF (left) and nonlinear NMF (right). We apply the nonlinear NMF (KNESC-Ncut) (35) with Gaussian kernel (right) and linear NMF introduced in [1] to the synthetic data set composed of two rings and denote the cluster memberships with different colors. The nonlinear NMF is able to produce the nonlinear separating hypersurfaces between the two rings.

will derive a practical method to solve this problem, and keep the rigorous orthogonality imposed on the clustering matrix. Following [7] we restrict \mathbf{W} to be a linear combination of transformed input data points, i.e., assume that \mathbf{W} lies in the column space of $\Phi(\mathbf{X})$

$$\mathbf{W} = \Phi(\mathbf{X})\mathbf{F} \quad (16)$$

The equation (16) can be interpreted as a simple transformation to the new basis, leading to the following minimization problem

$$\min_{\mathbf{H}, \mathbf{F} \geq 0} \|\Phi(\mathbf{X}) - \Phi(\mathbf{X})\mathbf{F}\mathbf{H}\|_F^2, \quad s.t. \quad \mathbf{H}\mathbf{H}^T = \mathbf{I} \quad (17)$$

120 The optimization problem of Eq. (17) is convex in either \mathbf{F} or \mathbf{H} , but not in both, meaning that the
 121 algorithm can only guarantee convergence to a local minimum [46]. The standard way to optimize (17)
 122 is to adopt an iterative, two-step strategy to alternatively optimize (\mathbf{F}, \mathbf{H}) . At each iteration, one of the
 123 matrices (\mathbf{F}, \mathbf{H}) is optimized while the other one is fixed. The resulting multiplicative update rules with
 124 explicitly included orthogonality constraints are obtained as

$$H_{ij} \leftarrow H_{ij} \frac{(\alpha \mathbf{F}^T \mathbf{K} + 2\mu \mathbf{H})_{ij}}{(\alpha \mathbf{F}^T \mathbf{K} \mathbf{F} \mathbf{H} + 2\mu \mathbf{H} \mathbf{H}^T \mathbf{H})_{ij}} \quad (18)$$

$$F_{jl} \leftarrow F_{jl} \frac{(\mathbf{K} \mathbf{H}^T)_{jl}}{(\mathbf{K} \mathbf{F} \mathbf{H} \mathbf{H}^T)_{jl}} \quad (19)$$

125 where $\mathbf{K} \in \mathbb{R}^{n \times n}$ is the kernel matrix [47, 48] defined as $\mathbf{K} \equiv \Phi^T(\mathbf{X})\Phi(\mathbf{X})$, where $\Phi(\mathbf{X})$ is a feature
 126 matrix in a nonlinear infinite-dimensional feature space.

We discuss two issues: (i) convergence of the algorithm, (ii) correctness of the converged solution.
Correctness. The correctness of the solution is assured by the fact that the solution at convergence

will satisfy the Karush-Kahn-Tucker (KKT) conditions for (17). The Lagrangian \mathcal{L} of the the above optimization problem (17) is

$$\mathcal{L} = \alpha \text{Tr}[\Phi(\mathbf{X})\Phi^\top(\mathbf{X})] - 2\alpha \text{Tr}[\Phi(\mathbf{X})\mathbf{F}\mathbf{H}\Phi^\top(\mathbf{X})] + \alpha \text{Tr}[\Phi(\mathbf{X})\mathbf{F}\mathbf{H}\mathbf{H}^\top\mathbf{F}^\top\Phi^\top(\mathbf{X})] + \mu \|\mathbf{H}\mathbf{H}^\top - \mathbf{I}_k\|_F^2 \quad (20)$$

By computing the partial derivatives of (20) with respect to \mathbf{H} and \mathbf{F} , we obtain

$$\frac{\partial \mathcal{L}}{\partial \mathbf{H}} = -2\alpha \mathbf{F}^\top \Phi^\top(\mathbf{X})\Phi(\mathbf{X}) + 2\alpha \mathbf{F}^\top \Phi^\top(\mathbf{X})\Phi(\mathbf{X})\mathbf{F}\mathbf{H} + 4\mu \mathbf{H}(\mathbf{H}^\top\mathbf{H} - \mathbf{I}_{n \times n}) \quad (21)$$

$$\frac{\partial \mathcal{L}}{\partial \mathbf{F}} = -\alpha \Phi^\top(\mathbf{X})\Phi(\mathbf{X})\mathbf{H}^\top + \alpha \Phi^\top(\mathbf{X})\Phi(\mathbf{X})\mathbf{F}\mathbf{H}\mathbf{H}^\top \quad (22)$$

Substituting the quadratic terms with the kernel matrix $\mathbf{K} = \Phi^\top(\mathbf{X})\Phi(\mathbf{X})$ yields

$$\alpha(\mathbf{F}^\top \mathbf{K} \mathbf{F} \mathbf{H} - \mathbf{F}^\top \mathbf{K}) + 2\mu \mathbf{H}(\mathbf{H}^\top \mathbf{H} - \mathbf{I}_{n \times n}) = 0 \quad (23)$$

$$-2\alpha \mathbf{K} \mathbf{H}^\top + 2\alpha \mathbf{K} \mathbf{F} \mathbf{H} \mathbf{H}^\top = 0 \quad (24)$$

Defining the Lagrange multiplier matrix for constraint $\mathbf{H} \geq 0$ as $\Psi = [\psi_{ij}]$ gives the KKT condition $\psi_{ij} H_{ij} = 0$. Similarly, the Lagrange multiplier matrix for constraint $\mathbf{F} \geq 0$ is given by $\Xi = [\xi_{jl}]$ and $\xi_{ij} F_{ij} = 0$. We obtain

$$[\alpha(\mathbf{F}^\top \mathbf{K} \mathbf{F} \mathbf{H} - \mathbf{F}^\top \mathbf{K}) + 2\mu \mathbf{H}(\mathbf{H}^\top \mathbf{H} - \mathbf{I}_{n \times n})]_{ij} H_{ij} = 0 \quad (25)$$

$$[2\alpha \mathbf{K} \mathbf{F} \mathbf{H} \mathbf{H}^\top - 2\alpha \mathbf{K} \mathbf{H}^\top]_{jl} F_{jl} = 0 \quad (26)$$

127 Separating positive and negative parts of the gradient leads to the multiplicative update rules (33)
128 and (32).

129 **Convergence.** The convergence is proved by following the auxiliary function method in [7, 31]. As
130 shown in [7], these update rules guarantee the decrease of the error and eventual convergence to local
131 minima. Note that in [7] a more general proof of the convergence can be obtained, for semi-nonnegative
132 matrix factorization, where input data matrix is negative $\mathbf{X} < 0$. We provide the proof for the convergence
133 in the Appendix B.

134 2.2. Kernel-based orthogonal NMF and spectral clustering

A connection between spectral clustering and factorization of the graph affinity matrix \mathbf{A} was demonstrated in [30] for Ncut spectral clustering, and for Rcut spectral clustering in [31]. It was also shown that the spectral clustering can be viewed as a factorization of the (scaled) data matrix itself [29]. Our question is whether the spectral clustering can be viewed as a non-negative factorization of the input

data matrix mapped to a nonlinear feature space. From Eq. (12) it can be seen that the Ncut spectral clustering is equivalent to the optimization problem

$$\max_{\mathbf{Z} \geq 0} \text{Tr} \left(\mathbf{Z} \mathbf{D}^{-1/2} \mathbf{A} \mathbf{D}^{-1/2} \mathbf{Z}^T \right) \quad \text{s.t.} \quad \mathbf{Z} \mathbf{Z}^T = \mathbf{I} \quad (27)$$

Theorem 1. Let $\mathbf{X} \geq 0$ denote the input data matrix. Let the similarity between the data points be defined as the inner product in the nonlinear feature space, i.e. the graph affinity matrix $\mathbf{A} = \Phi^T(\mathbf{X})\Phi(\mathbf{X})$. Then the k -way Ncut spectral clustering (27) is equivalent to the non-negative matrix factorization of the scaled input data matrix mapped to the nonlinear feature space $\Phi(\mathbf{X})\mathbf{D}^{-1/2} = \mathbf{W}\mathbf{Z}$ subject to $\mathbf{Z}\mathbf{Z}^T = \mathbf{I}$, where $\mathbf{W} = \Phi(\mathbf{X})\mathbf{F}$ and \mathbf{Z} and \mathbf{F} are two non-negative matrices, and the columns of \mathbf{Z} serve as a clustering indicator vector of each data point.

The proof of the Theorem 1 is given in the Appendix A. Theorem 1 shows that Ncut spectral clustering can be viewed as a nonlinear orthogonal NMF problem with the scaling factor $\mathbf{D}^{-1/2}$. For the Rcut spectral clustering we cannot obtain an exact equivalence. However, we can relax the Rcut spectral clustering and get an equivalence between the relaxed Rcut spectral clustering and nonlinear orthonormal NMF.

Theorem 2. Let $\mathbf{X} \geq 0$ denote the input data matrix. Let the similarity between the data points be defined by inner product in nonlinear feature space i.e. the affinity matrix $\mathbf{A} = \Phi^T(\mathbf{X})\Phi(\mathbf{X})$. Then the k -way relaxed Rcut spectral clustering (11) is equivalent to the non-negative matrix factorization of the data matrix $\Phi(\mathbf{X}) = \mathbf{W}\mathbf{H}$ subject to $\mathbf{H}\mathbf{H}^T = \mathbf{I}$, where $\mathbf{W} = \Phi(\mathbf{X})\mathbf{F}$ and \mathbf{H} and \mathbf{F} are two non-negative matrices, and the columns of \mathbf{H} serve as a clustering indicator vector of each data point.

The proof of the Theorem 2 is given in the Appendix A. Theorems 1 and 2 establish the nonlinear orthogonal NMF approach to non-negative spectral clustering. Our assumptions include that the similarity graph is fully connected and the similarity matrix \mathbf{A} is given by the kernel $\mathbf{K} = \Phi^T(\mathbf{X})\Phi(\mathbf{X})$. Similarly to this result, it was shown in [30] that the standard inner-product matrix $\mathbf{A} = \mathbf{X}^T\mathbf{X}$ can be extended to any other kernel by a nonlinear transformation to a higher dimensional space.

To solve Ncut and Rcut spectral clustering we employ the kernel-based multiplicative update rules with orthonormal constraints. Considering the equivalence and solving the two optimization problems we obtain *kernel-based non-negative spectral clustering* for Ncut (KNSC-Ncut)

$$\min_{\mathbf{Z}, \mathbf{F} \geq 0} \|\Phi(\mathbf{X})\mathbf{D}^{-1/2} - \Phi(\mathbf{X})\mathbf{F}\mathbf{Z}\|_F^2, \quad \text{s.t.} \quad \mathbf{Z}\mathbf{Z}^T = \mathbf{I} \quad (28)$$

with the following multiplicative update rule

$$Z_{ij} \leftarrow Z_{ij} \frac{(\alpha \mathbf{F}^T \mathbf{K} \mathbf{D}^{-1/2} + 2\mu \mathbf{Z})_{ij}}{(\alpha \mathbf{F}^T \mathbf{K} \mathbf{F} \mathbf{Z} + 2\mu \mathbf{Z} \mathbf{Z}^T \mathbf{Z})_{ij}} \quad (29)$$

$$F_{jl} \leftarrow F_{jl} \frac{(\mathbf{K} \mathbf{Z}^T)_{jl}}{(\mathbf{K} \mathbf{F} \mathbf{Z} \mathbf{Z}^T)_{jl}} \quad (30)$$

The parameter μ can be set so that the orthogonality of the matrix \mathbf{Z} is preserved during the updates. An exact orthogonality of the clustering matrix \mathbf{Z} implies each column of \mathbf{Z} can have only one non-zero element, which implies that each data object belongs only to one cluster. This is hard clustering, such as in k -means [30, 5]. Furthermore, KNSC-Ncut has a soft clustering interpretation [1, 31, 30] where a data point could belong fractionally to more than one cluster. The soft clustering membership of data point \mathbf{x}_i to cluster j can be defined as a probability distribution $c_{i,j} = \mathbf{Z}_{ji} / \sum_k \mathbf{Z}_{ki}$. We summarize the KNSC-Ncut algorithm in the Algorithm 1. Similarly, the optimization problem for *kernel-based non-negative spectral clustering* for Rcut (KNSC-Rcut)

$$\min_{\mathbf{H}, \mathbf{F} \geq 0} \|\Phi(\mathbf{X}) - \Phi(\mathbf{X})\mathbf{F}\mathbf{H}\|_F^2, \quad s.t. \quad \mathbf{H}\mathbf{H}^\top = \mathbf{I} \quad (31)$$

gives the multiplicative update rule for KNSC-Rcut

$$H_{ij} \leftarrow H_{ij} \frac{(\alpha \mathbf{F}^\top \mathbf{K} + 2\mu \mathbf{H})_{ij}}{(\alpha \mathbf{F}^\top \mathbf{K} \mathbf{F} \mathbf{H} + 2\mu \mathbf{H} \mathbf{H}^\top \mathbf{H})_{ij}} \quad (32)$$

$$F_{jl} \leftarrow F_{jl} \frac{(\mathbf{K} \mathbf{H}^\top)_{jl}}{(\mathbf{K} \mathbf{F} \mathbf{H} \mathbf{H}^\top)_{jl}} \quad (33)$$

and summarize the KNSC-Rcut algorithm in Algorithm 2.

Algorithm 1 Kernel-based non-negative spectral clustering for Ncut (KNSC-Ncut)

Input: $\mathbf{X} \in \mathbb{R}^{m \times n}$, $\mathbf{K} \in \mathbb{R}^{n \times n}$, $\mathbf{A} \in \mathbb{R}^{n \times n}$, number of clusters k

Output: clustering matrix $\mathbf{Z} \in \mathbb{R}^{k \times n}$, vector of cluster memberships $c_i = \operatorname{argmax}_{1 \leq j \leq k} \mathbf{Z}_{ji}$

Initialize two non-negative matrices $\mathbf{Z} \in \mathbb{R}^{k \times n}$ and $\mathbf{F} \in \mathbb{R}^{n \times k}$ with random numbers generated in the range $[0, 1]$.

Calculate the degree matrix $\mathbf{D} = \operatorname{diag}(d_1, \dots, d_n)$

$$d_i = \sum_{j=1}^n A_{ij} \quad (34)$$

repeat

$$Z_{ij} \leftarrow Z_{ij} \frac{(\alpha \mathbf{F}^\top \mathbf{K} \mathbf{D}^{-1/2} + 2\mu \mathbf{Z})_{ij}}{(\alpha \mathbf{F}^\top \mathbf{K} \mathbf{F} \mathbf{Z} + 2\mu \mathbf{Z} \mathbf{Z}^\top \mathbf{Z})_{ij}}$$

$$F_{jl} \leftarrow F_{jl} \frac{(\mathbf{K} \mathbf{Z}^\top)_{jl}}{(\mathbf{K} \mathbf{F} \mathbf{Z} \mathbf{Z}^\top)_{jl}}$$

until Stopping criterion is reached

157

158 The convergence of the multiplicative update rules (29)–(30), and (32)–(33), has been proved in

159 Appendix B by the auxiliary function method. These update rules guarantee the decrease of error and

Algorithm 2 Kernel-based non-negative spectral clustering for Rcut (KNSC-Rcut)

Input: $\mathbf{X} \in \mathbb{R}^{m \times n}$, $\mathbf{K} \in \mathbb{R}^{n \times n}$, number of clusters k

Output: clustering matrix $\mathbf{H} \in \mathbb{R}^{k \times n}$, vector of cluster memberships $c_i = \underset{1 \leq j \leq k}{\operatorname{argmax}} \mathbf{H}_{ji}$

Initialize two non-negative matrices $\mathbf{H} \in \mathbb{R}^{k \times n}$ and $\mathbf{F} \in \mathbb{R}^{n \times k}$ with random numbers generated in the range $[0, 1]$.

repeat

$$H_{ij} \leftarrow H_{ij} \frac{(\alpha \mathbf{F}^\top \mathbf{K} + 2\mu \mathbf{H})_{ij}}{(\alpha \mathbf{F}^\top \mathbf{K} \mathbf{F} \mathbf{H} + 2\mu \mathbf{H} \mathbf{H}^\top \mathbf{H})_{ij}}$$

$$F_{jl} \leftarrow F_{jl} \frac{(\mathbf{K} \mathbf{H}^\top)_{jl}}{(\mathbf{K} \mathbf{F} \mathbf{H} \mathbf{H}^\top)_{jl}}$$

until Stopping criterion is reached

160 eventually converge to a local minima [7]. In our experiments, we have set the maximum amount of
 161 iterations to 300 (usually 100 iterations are enough) and we use the convergence rule $E_{i-1} - E_i \leq$
 162 $\kappa \max(1, E_{i-1})$ in order to stop the updates when the reconstruction error (E_i) between the current and
 163 previous update is small enough. We have set the $\kappa = 10^{-3}$.

164 The two proposed algorithms have a run-time complexity of $\mathcal{O}(kn^2)$ for clustering n data points to
 165 k clusters, which is less than standard spectral clustering methods $\mathcal{O}(n^3)$ and the same complexity as
 166 the state-of-the-art methods [29, 32, 35]. The main advantage of the kernel-based NMF approach is
 167 that it can be easily optimized to achieve higher clustering accuracy for the data drawn from nonlinear
 168 manifolds, avoiding the computation of eigenvalues and eigenvectors.

169 2.3. Graph regularized kernel-based orthogonal NMF

A non-negative matrix factorization that respects the geometric structure of the data in the nonlinear feature space can be constructed by introducing an additional graph regularization term into the objective function (17). Recall that our nonlinear NMF tries to find a set of basis vectors that can be used to best approximate the data $\Phi(\mathbf{X}) = \mathbf{W}\mathbf{H}$. Let \mathbf{h}_j denote the j -th column of \mathbf{H} , $\mathbf{h}_j = [h_{j1}, \dots, h_{jk}]$, then \mathbf{h}_j can be regarded as the new representation of the j -th data point with respect to the new basis $\mathbf{W} = \Phi(\mathbf{X})\mathbf{F}$. The graph regularization term can be viewed as a local invariance assumption [41, 49, 50], which states that if two data points $\Phi(\mathbf{x}_i)$ and $\Phi(\mathbf{x}_j)$ are close to each other in the original geometry of the data distribution, then \mathbf{h}_j and \mathbf{h}_l , the low dimensional representations of these two points, are also close to each other. This can be written as

$$\mathcal{R} = \frac{1}{2} \sum_{j,l=1}^n \|\mathbf{h}_j - \mathbf{h}_l\|_F^2 \mathbf{A}_{jl} = \sum_{j=1}^n \mathbf{h}_j \mathbf{h}_j^\top \mathbf{D}_{j,j} - \sum_{j,l=1}^n \mathbf{h}_j \mathbf{h}_l^\top \mathbf{A}_{j,l} = \operatorname{Tr}(\mathbf{H} \mathbf{L} \mathbf{H}^\top) \quad (35)$$

By minimizing the regularization term \mathcal{R} with respect to \mathbf{H} , we expect that when $\Phi(\mathbf{x}_i)$ and $\Phi(\mathbf{x}_j)$ are close (*i.e.* when \mathbf{A}_{jl} is large) the points \mathbf{h}_j and \mathbf{h}_l are also close with respect to the new basis. The

objective function for nonlinear orthogonal graph regularized NMF is given as

$$\min_{\mathbf{H}, \mathbf{F} \geq 0} \alpha \|\Phi(\mathbf{X}) - \Phi(\mathbf{X})\mathbf{F}\mathbf{H}\|_F^2 + \lambda \text{Tr}(\mathbf{H}\mathbf{L}\mathbf{H}^\top), \text{ s.t. } \mathbf{H}\mathbf{H}^\top = \mathbf{I} \quad (36)$$

By adopting the same iterative procedure to alternatively fix one of the matrices \mathbf{F} and \mathbf{H} , we solve the minimization problem (36) and obtain the multiplicative update rules

$$H_{ij} \leftarrow H_{ij} \frac{(\alpha \mathbf{F}^\top \mathbf{K} + 2\mu \mathbf{H} + \lambda \mathbf{H}\mathbf{A})_{ij}}{(\alpha \mathbf{F}^\top \mathbf{K}\mathbf{F}\mathbf{H} + 2\mu \mathbf{H}\mathbf{H}^\top \mathbf{H} + \lambda \mathbf{H}\mathbf{D})_{ij}} \quad (37)$$

$$F_{jl} \leftarrow F_{jl} \frac{(\mathbf{K}\mathbf{H}^\top)_{jl}}{(\mathbf{K}\mathbf{F}\mathbf{H}\mathbf{H}^\top)_{jl}} \quad (38)$$

170 where \mathbf{K} is the kernel matrix. There are many choices to define the weight matrix \mathbf{A} of the graph.
 171 For example, the scalar product weighting and the cosine similarity are most suitable for processing
 172 documents, while for image data the heat kernel is commonly used [51, 4, 41]. We will use the fully
 173 connected affinity graph with the Gauss kernel weighting, as we do not treat different weighting schemes
 174 separately.

Correctness. The correctness of the solution is assured by the fact that the solution at convergence will satisfy the KKT conditions for the optimization problem (36). The Lagrangian \mathcal{L} of the the optimization problem (36) can be written as

$$\begin{aligned} \mathcal{L} = & \alpha \text{Tr}[\Phi(\mathbf{X})\Phi^\top(\mathbf{X})] - 2\alpha \text{Tr}[\Phi(\mathbf{X})\mathbf{F}\mathbf{H}\Phi^\top(\mathbf{X})] + \alpha \text{Tr}[\Phi(\mathbf{X})\mathbf{F}\mathbf{H}\mathbf{H}^\top \mathbf{F}^\top \Phi^\top(\mathbf{X})] + \\ & + \mu \|\mathbf{H}\mathbf{H}^\top - \mathbf{I}_k\|_F^2 + \lambda \text{Tr}[\mathbf{H}\mathbf{D}\mathbf{H}^\top] - \lambda \text{Tr}[\mathbf{H}\mathbf{A}\mathbf{H}^\top] \end{aligned} \quad (39)$$

We calculate the partial derivatives of (39) with respect to \mathbf{H} and \mathbf{F}

$$\frac{\partial \mathcal{L}}{\partial \mathbf{H}} = -2\alpha \mathbf{F}^\top \Phi^\top(\mathbf{X})\Phi(\mathbf{X}) + 2\alpha \mathbf{F}^\top \Phi^\top(\mathbf{X})\Phi(\mathbf{X})\mathbf{F}\mathbf{H} + 4\mu \mathbf{H}(\mathbf{H}^\top \mathbf{H} - \mathbf{I}_{n \times n}) + 2\lambda \mathbf{H}\mathbf{D} - 2\lambda \mathbf{H}\mathbf{A} \quad (40)$$

$$\frac{\partial \mathcal{L}}{\partial \mathbf{F}} = -\alpha \Phi^\top(\mathbf{X})\Phi(\mathbf{X})\mathbf{H}^\top + \alpha \Phi^\top(\mathbf{X})\Phi(\mathbf{X})\mathbf{F}\mathbf{H}\mathbf{H}^\top \quad (41)$$

Substituting the quadratic terms with kernel matrix gives

$$\alpha(\mathbf{F}^\top \mathbf{K}\mathbf{F}\mathbf{H} - \mathbf{F}^\top \mathbf{K}) + 2\mu \mathbf{H}(\mathbf{H}^\top \mathbf{H} - \mathbf{I}_{n \times n}) + \lambda \mathbf{H}\mathbf{L} = 0 \quad (42)$$

$$-2\alpha \mathbf{K}\mathbf{H}^\top + 2\alpha \mathbf{K}\mathbf{F}\mathbf{H}\mathbf{H}^\top = 0 \quad (43)$$

Defining the Lagrange multiplier matrix for constraint $\mathbf{H} \geq 0$ as $\Psi = [\psi_{ij}]$, the KKT condition is $\psi_{ij}H_{ij} = 0$. Similarly, the Lagrange multiplier matrix for constraint $\mathbf{F} \geq 0$ is given by $\Xi = [\xi_{jl}]$ and we obtain

$$[\alpha(\mathbf{F}^\top \mathbf{K}\mathbf{F}\mathbf{H} - \mathbf{F}^\top \mathbf{K}) + 2\mu \mathbf{H}(\mathbf{H}^\top \mathbf{H} - \mathbf{I}_{n \times n}) + \lambda \mathbf{H}\mathbf{L}]_{ij} H_{ij} = 0$$

$$[2\alpha\mathbf{K}\mathbf{F}\mathbf{H}\mathbf{H}^\top - 2\alpha\mathbf{K}\mathbf{H}^\top]_{jl}F_{jl} = 0 \quad (44)$$

175 We separate positive and negative parts of the gradient and obtain multiplicative update rules (37) and
 176 (38). By setting $\lambda = 0$ the update rules in Eq. (37) and (38) reduce to the update rules of the KONMF.
 177 We summarize the graph regularized kernel-based orthogonal NMF in the Algorithm 3.

Algorithm 3 Kernel-based orthogonal graph regularized NMF (KOGNMF)

Input: $\mathbf{X} \in \mathbb{R}^{m \times n}$, number of clusters k , $\mathbf{K} \in \mathbb{R}^{n \times n}$, $\mathbf{A} \in \mathbb{R}^{n \times n}$

Output: clustering matrix \mathbf{H} , vector of cluster memberships $c_i = \operatorname{argmax}_{1 \leq j \leq k} \mathbf{H}_{ji}$

Initialize two non-negative matrices $\mathbf{H} \in \mathbb{R}^{k \times n}$ and $\mathbf{F} \in \mathbb{R}^{n \times k}$ with random numbers generated in the range $[0, 1]$.

Calculate the degree matrix $\mathbf{D} = \operatorname{diag}(d_1, \dots, d_n)$

$$d_i = \sum_{j=1}^n A_{ij}$$

repeat

$$H_{ij} \leftarrow H_{ij} \frac{(\alpha\mathbf{F}^\top\mathbf{K} + 2\mu\mathbf{H} + \lambda\mathbf{H}\mathbf{A})_{ij}}{(\alpha\mathbf{F}^\top\mathbf{K}\mathbf{F}\mathbf{H} + 2\mu\mathbf{H}\mathbf{H}^\top\mathbf{H} + \lambda\mathbf{H}\mathbf{D})_{ij}}$$

$$F_{jl} \leftarrow F_{jl} \frac{(\mathbf{K}\mathbf{H}^\top)_{jl}}{(\mathbf{K}\mathbf{F}\mathbf{H}\mathbf{H}^\top)_{jl}}$$

until Stopping criterion is reached

178 The proposed algorithm has two additional matrix multiplications $\mathbf{H}\mathbf{A}$ and $\mathbf{H}\mathbf{D}$ with complexity of
 179 $O(kn^2)$. Therefore, the total run-time complexity is unchanged and equal to $O(kn^2)$ for clustering n data
 180 points to k clusters. The convergence proof for the multiplicative updates (37)-(38) can be found in the
 181 Appendix B.

182 3. Experiments

183 In this section we carry out extensive experiments on synthetic and real world data sets to illustrate
 184 the effectiveness of the three proposed algorithms: KNSC-Ncut, KNSC-Rcut and KOGNMF. We compare
 185 nine recently proposed non-negative spectral clustering algorithms [29, 31, 32] and traditional Ncut and
 186 Rcut spectral clustering methods [19, 26]. Our experimental setting is similar to [29, 32]. For the purpose
 187 of reproducibility we provide the code and data sets (see supplementary files).

188 3.1. Data sets and the evaluation metric

189 We have used the same data sets as in [29, 30, 32]: five UCI [52] data sets and AT&T face database
 190 [53]. The UCI datasets are Soybean, Zoo, Glass, Dermatology and Vehicle. The AT&T face database
 191 consists of gray scale face images of 40 persons. Each person has 10 facial images under different light and
 192 illumination conditions and the images from the same person belong to the same cluster. The important
 193 statistics of these data sets are summarized in the Table 2, including the number of samples, dimensions
 194 and the number of clusters.

Table 2: Features of the UCI and AT&T data sets

Datasets	Samples	Dimension	Clusters
Soybean	47	35	4
Zoo	101	16	7
AT&T	400	10304	40
Glass	214	9	6
Dermatology	366	33	6
Vehicle	846	18	4

The clustering accuracy is evaluated by the common clustering accuracy measure [29, 31, 32], which computes the percentage of data points that are correctly clustered with respect to the external ground truth labels. For each data point \mathbf{x}_i its label is denoted with c_i and the ground truth cluster index with g_i . In order to calculate the optimal assignment of labels to cluster indices $f(c_i)$, the Hungarian bipartite matching algorithm [52] is used, with the complexity $O(k^3)$ for k clusters. The clustering accuracy can be expressed as:

$$ACC = \frac{\sum_{i=1}^n \delta(g_i, f(c_i))}{n}, \quad (45)$$

where n denotes the total number of data points and the δ function is defined as

$$\delta(g_i, c_i) = \begin{cases} 1 & : g_i = f(c_i), \\ 0 & : g_i \neq f(c_i). \end{cases}$$

195 3.2. Compared algorithms

196 We compare our methods to nine recently proposed non-negative spectral clustering approaches and
 197 traditional spectral clustering Ncut and Rcut methods:

- 198 • Normalized cut (Ncut) and ratio cut (Rcut) spectral clustering. Ncut spectral clustering exists
 199 in different normalizations [19, 28]. Our implementation is according to Ncut from [19], where
 200 eigenvectors of normalized Laplacian matrix \mathbf{Z} are normalized such that the L_2 norm of each row
 201 equals 1.

- 202 • Non-negative spectral clustering methods NSC-Ncut, NSC-Rcut, and non-negative sparse spectral
203 clustering methods NSSC-Ncut and NSSC-Rcut from [29].
- 204 • Global discriminative-based nonnegative spectral clustering methods [32] GDBNSC-Ncut and GDBNSC-
205 Rcut.
- 206 • Symmetric NMF for spectral clustering [31] (NLE). This is the symmetric NMF of the pairwise
207 affinity matrix, which is originally implemented as the standard inner product linear kernel matrix
208 $\mathbf{A} = \mathbf{X}^T \mathbf{X}$.

209 3.3. Clustering results

210 We perform $n = 256$ independent runs with random initializations for each of the proposed methods
211 KNSC-Ncut, KNSC-Rcut and KOGNMF. In each run, we randomly initialize matrices $(\mathbf{H}, \mathbf{Z}, \mathbf{F})$ and
212 then iterate multiplicative update rules to achieve convergence and obtain cluster indicator matrix. In all
213 experiments we have used 300 iterations and the convergence occurred after approximately 100 iterations.
214 The cluster memberships for each data point i is obtained by taking the index of the maximal value of
215 i -th column in the orthogonal clustering matrix \mathbf{H} (or \mathbf{Z}). For the Rcut and Ncut, the first k eigenvectors
216 are computed once and then 256 runs of k -means are performed.

217 In Fig. 2 we plot the clustering performance of the NSC-Ncut and KNSC-Ncut on two-dimensional
218 synthetic examples. The synthetic example demonstrates the ability of KNSC-Ncut to separate the
219 nonlinear clusters with high clustering accuracy. In Fig. 3, 4 and 5 we plot the average clustering
220 accuracy over 256 runs on the six data sets. The average clustering accuracy is reported for independent
221 number of runs 2^i , where $i = 1, 2, \dots, 8$. The average clustering accuracy for the Ncut group of algorithms
222 is plotted in the Fig. 3. In the Fig. 4 the average clustering accuracy is plotted for the Rcut group.²
223 The average clustering accuracy of KOGNMF is shown in Fig. 5. We summarize the average clustering
224 accuracy results for the Ncut and the Rcut group of algorithms in Table 3. On data sets Dermatology,
225 Glass, Zoo and AT&T, the KNSC-Ncut clustering accuracy is improved and KNSC-Ncut outperforms
226 Ncut, NSC-Ncut, NSSC-Ncut and GDBNSC-Ncut. On the high dimensional AT&T face database the
227 clustering accuracy of the KNSC-Ncut algorithm shows considerable improvement. On the Soybean and
228 Vehicle data sets the KNSC-Ncut is comparable with the GDBNSC-Ncut. Similarly, on Dermatology,
229 Glass, Zoo, Vehicle and AT&T data set, KNSC-Rcut outperforms Rcut, NSC-Rcut, NSSS-Rcut and
230 GDBNSC-Rcut. In Fig. 5 we plot the average clustering accuracy for the KOGNMF algorithm. The
231 KOGNMF considerably outperforms all algorithms on every data set (Table 3).

²The results in Table 3 for the GDBNSC method are reported from original work [32], however in Fig. 3, 4 and 5 the results for this method were omitted due to the numerical instabilities in reproduction of this method with reported parameters [32].

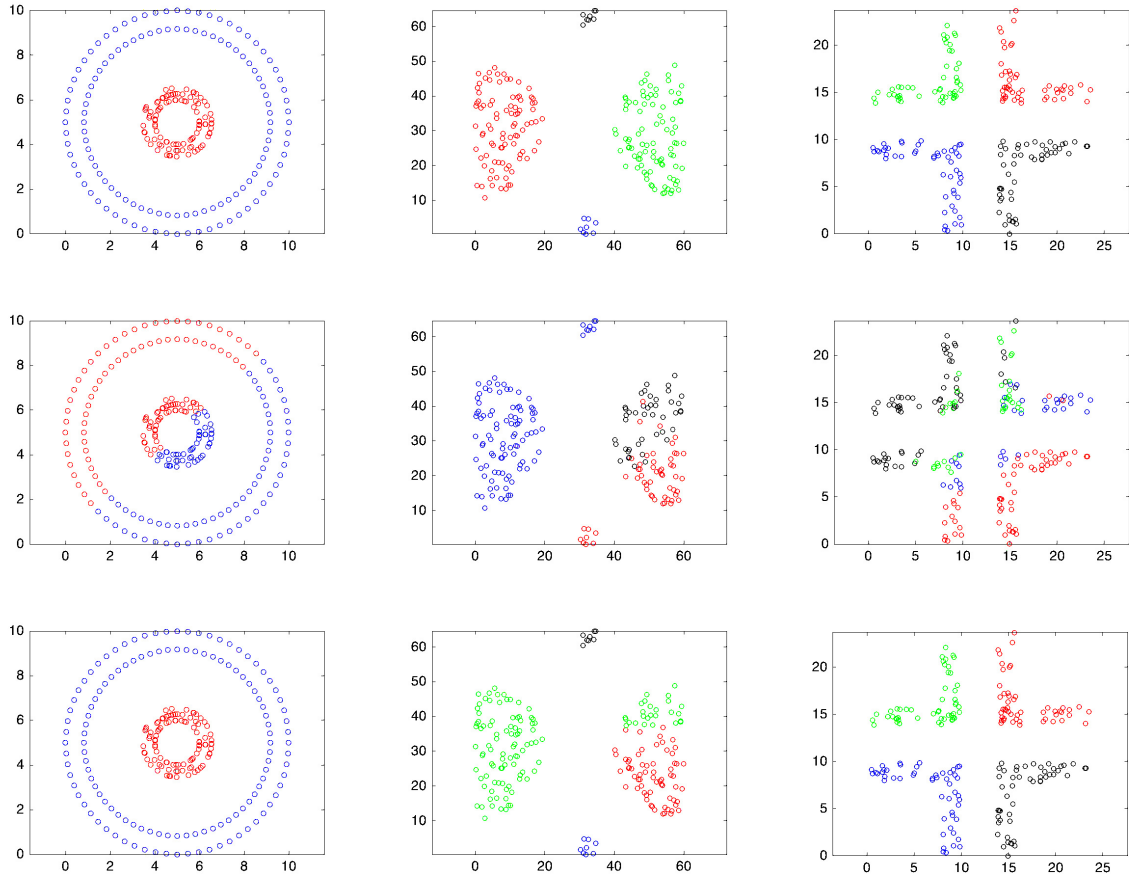


Figure 2: The optimized clustering results of the KNSC-Ncut algorithm compared with the optimized clustering results of the NSC-Ncut [29]. The two-dimensional data sets with 2 and 4 clusters are plotted in the first row, different clusters are represented with different colors. In the second row we plot the clustering results of the NSC-Ncut. The clustering results of the KNSC-Ncut algorithm are plotted in the third row. The clustering accuracy over 256 independent runs is 0.5, 0.7 and 0.62 for NSC-Ncut, and 0.90, 0.85 and 0.82 for the KNSC-Ncut, for the three data sets respectively. The KNSC-Ncut is able to separate the nonlinear data set composed of two rings of points with high clustering accuracy.

Table 3: *The average clustering accuracy on 5 UCI and AT&T data sets*

	Dermatology	Glass	Soybean	Zoo	Vehicle	AT&T
Ncut	0.75	0.46	0.70	0.63	0.37	0.62
NSC-Ncut	0.71	0.25	0.71	0.61	0.39	0.35
NSSC-Ncut	0.71	0.34	0.71	0.66	0.41	0.02
GDBNSC-Ncut	0.82	0.41	0.79	0.65	0.46	0.38
KNSC-Ncut	0.87	0.50	0.78	0.80	0.45	0.70
Rcut	0.47	0.41	0.63	0.60	0.33	0.31
NSC-Rcut	0.66	0.25	0.69	0.61	0.38	0.35
NLE	0.34	0.25	0.47	0.49	0.28	0.20
NSSC-Rcut	0.67	0.26	0.69	0.61	0.38	0.35
GDBNSC-Rcut	0.73	0.36	0.80	0.64	0.388	0.36
KNSC-Rcut	0.87	0.45	0.75	0.65	0.45	0.69
KOGNMF	0.91	0.48	0.80	0.78	0.45	0.70

Table 3: The average clustering accuracy of KNSC-Ncut, KNSC-Rcut and KOGNMF compared with 9 recently proposed NMF-based NSC methods on the 5 UCI [52] data sets and the AT&T face database [53]. KNSC-Rcut performs considerably better on 4 data sets, and has a comparable accuracy on two data sets. KNSC-Ncut algorithm outperforms on 5 data sets, and has a comparable clustering accuracy on one data set. KOGNMF algorithm has considerably better accuracy on 4 data sets, including the difficult AT&T face images database, and is comparable on two data sets. All three algorithms have considerably higher clustering accuracy on the difficult AT&T face database.

Table 4: *The average clustering accuracy on the hold-out validation set*

Datasets	Dermatology	Glass	Soybean	Zoo	Vehicle	AT&T
NLE	0.37	0.38	0.55	0.45	0.33	0.26
KNSC-Ncut	0.87	0.47	0.73	0.77	0.47	0.70
KNSC-Rcut	0.85	0.47	0.76	0.67	0.48	0.73
KOGNMF	0.89	0.49	0.76	0.78	0.48	0.73

Table 4: The hold-out validation consists of randomly splitting each data set into two equally sized parts with the equally distributed cluster membership. The grid search optimization is performed on the first half of the data set, while the second half is used as a hold-out validation where optimized parameters are used. For each data set, we measure the average score over 256 independent runs on the hold-out data. We denote with bold our results that outperform the optimized clustering accuracy scores of the state-of-the-art NSC methods without the hold-out validation. The KNSC-Ncut and KNSC-Rcut algorithms have higher average clustering accuracy on the majority of data sets, while KOGNMF algorithm outperforms on all six data sets.

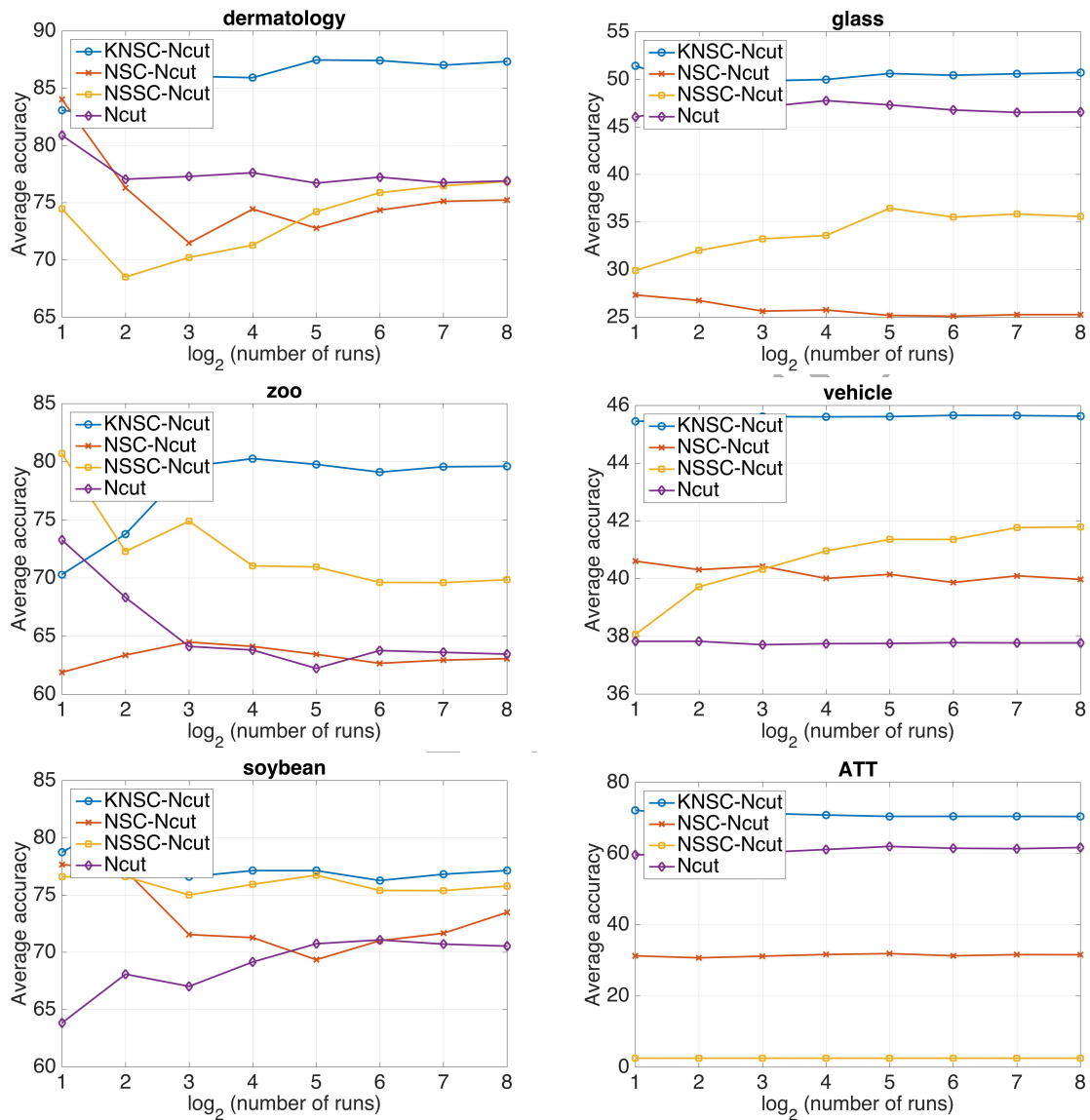


Figure 3: The average clustering accuracy of KNSC-Ncut algorithm compared with Ncut, NSC-Ncut and NSSC-Ncut algorithms on five UCI [52] data sets and AT&T face database [53]. The average clustering accuracy is plotted for the independent number of runs $2^i = \{2, 4, \dots, 256\}$. The clustering accuracy of KNSC-Ncut is higher on the majority of data sets. The clustering accuracy for the AT&T face database is considerably improved when compared with the state-of-the-art non-negative spectral clustering methods.

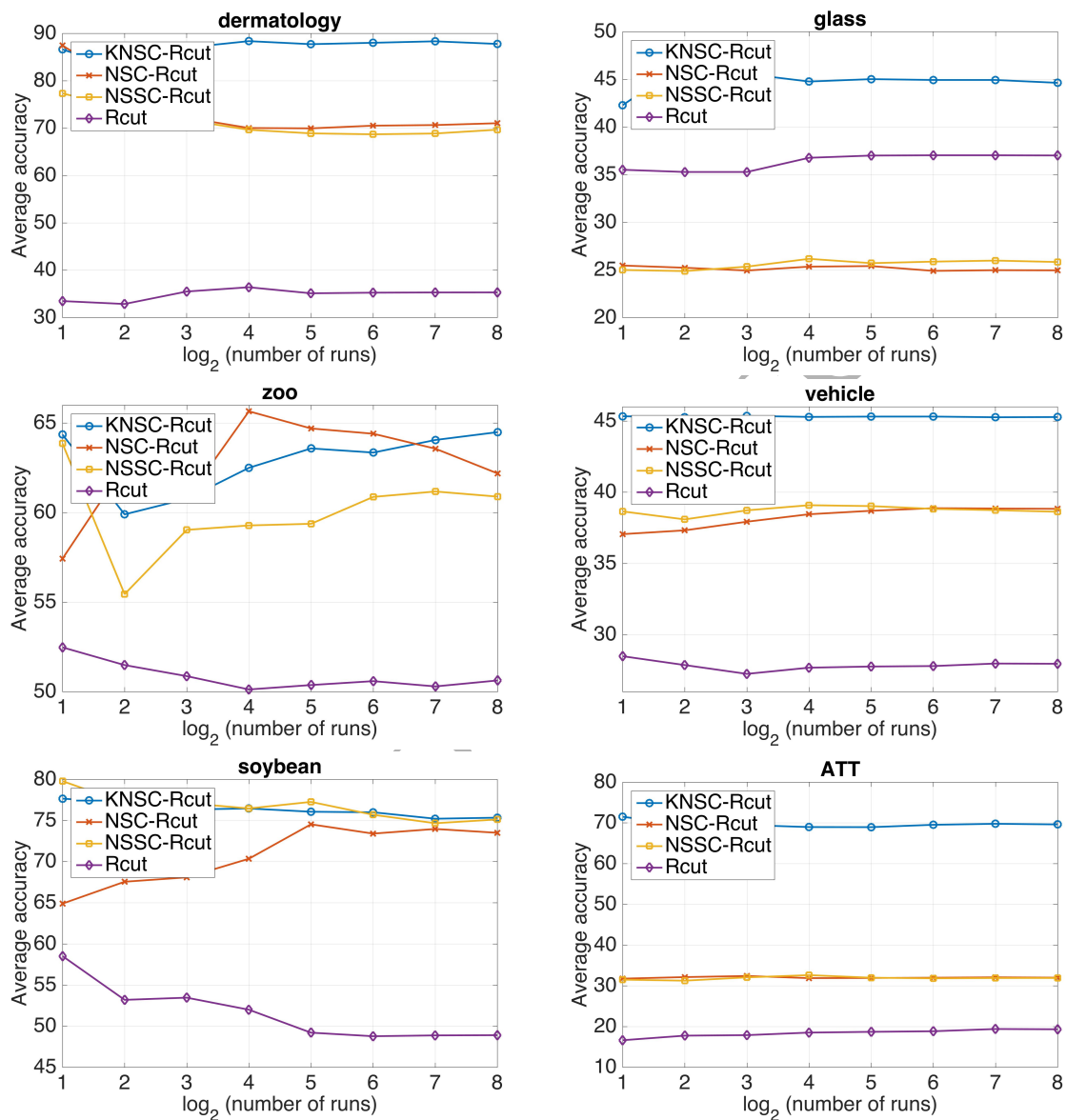


Figure 4: The average clustering accuracy of KNSC-Rcut algorithm compared with Rcut, NSC-Rcut and NSSC-Rcut algorithms on five UCI [52] data sets and AT&T face database [53]. The average clustering accuracy is plotted for the independent number of runs $2^i = \{2, 4, \dots, 256\}$. The KNSC-Rcut algorithm outperforms NSC algorithms on the majority of data sets.

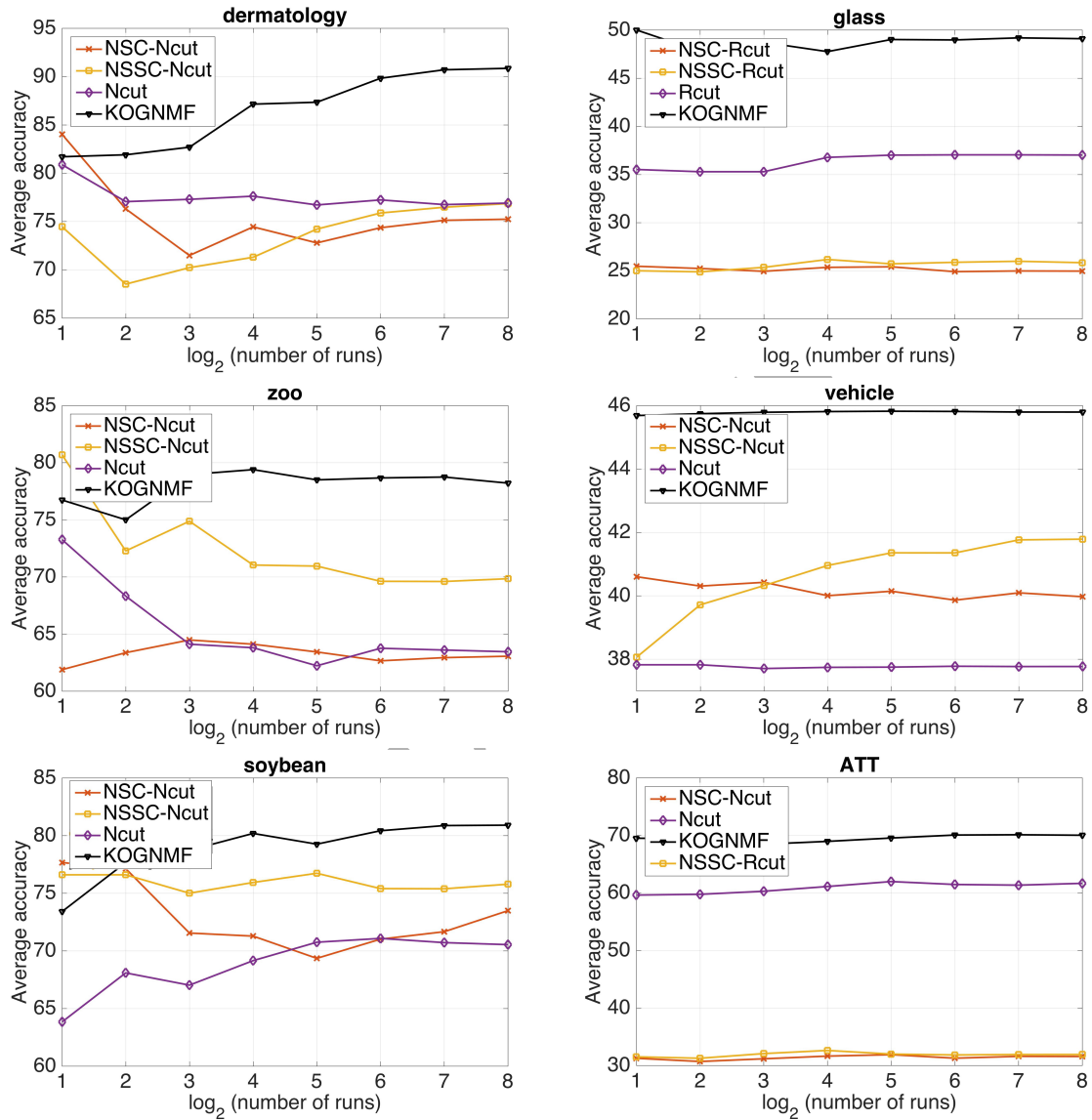


Figure 5: The average clustering accuracy of KOGNMF algorithm on 5 UCI [52] data sets and AT&T face database. The average clustering accuracy is plotted for the independent number of runs $2^i = \{2, 4, \dots, 256\}$. The KOGNMF algorithm outperforms all non-negative spectral clustering methods on every data set, including the difficult AT&T face database [53].

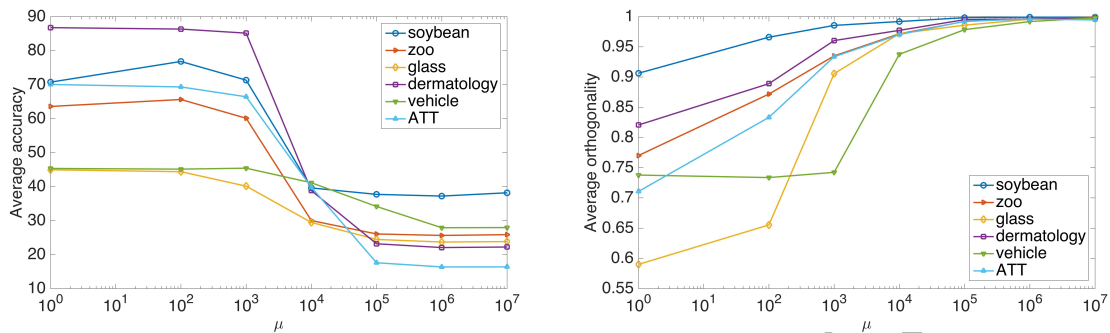


Figure 6: Left: The average orthogonality of the clustering matrix \mathbf{H} (KNSC-Rcut) over the 256 runs, plotted for fixed reconstruction error parameter $\alpha = 10$ and for a wide range of values of the orthogonality parameter μ on all six data sets. Right: The average clustering accuracy of KNSC-Rcut for fixed $\alpha = 10$ plotted for different values of the parameter μ . The average orthogonality of the clustering matrix \mathbf{H} increases up to 1 if the parameter μ is increased. The average clustering accuracy is robust for all six data sets for a wide range of the trade-off parameter μ .

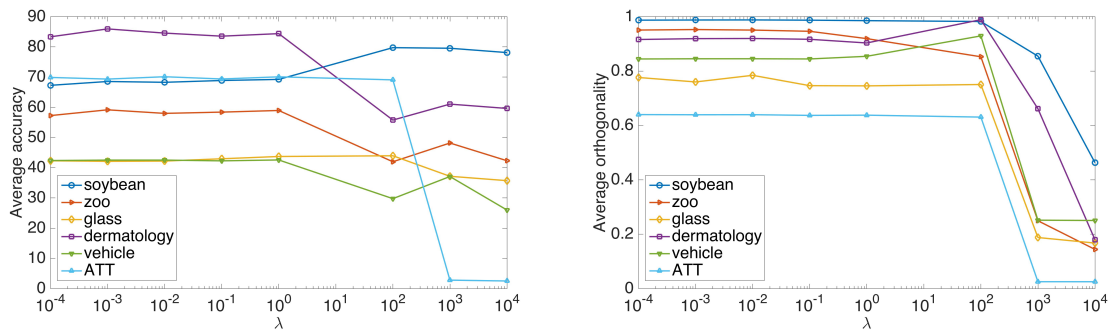


Figure 7: Left: The average orthogonality of the clustering matrix \mathbf{H} (KNSC-Rcut) over the 256 runs, plotted for fixed reconstruction error parameter $\alpha = 10$ and orthogonality regularization parameter $\mu = 100$ for different values of the graph regularization parameter λ on all six data sets. Right: The average clustering accuracy of KNSC-Rcut for fixed parameters $\alpha = 10$ and $\mu = 100$ plotted for different values of the parameter λ . The average clustering accuracy is robust for all six data sets for a wide range of the trade-off parameter λ .

232 3.4. The parameter selection

233 The kernel-based orthogonal NMF multiplicative rules have in total four parameters: α , μ and λ and
 234 the Gaussian kernel width σ . The three parameters α , μ and λ are a trade-off parameters which balance
 235 the reconstruction error, orthogonality regularization and the graph regularization, respectively. In all
 236 the experiments and data sets we have fixed the three trade-off parameters to the same constant values
 237 $\alpha = 10$, $\mu = 100$ and $\lambda = 10$. Furthermore, the three trade-off parameters can be reduced to two, as the
 238 NMF objective functions given in the Eqs. (17) and (36) can be divided by α . By fixing the trade-off
 239 parameters throughout all of the experiments we effectively need to optimize only one parameter, which
 240 is the kernel width. For the trade-off parameters we perform sensitivity analysis to demonstrate that
 241 the constant values of the trade-off parameters can be chosen in a wide range of values (a few orders of
 242 magnitude), as shown in Fig. 6 and 7.

243 In the experiments we use the Gaussian kernel defined as $\mathbf{K}(\mathbf{x}_i, \mathbf{x}_j) = \exp(-\|\mathbf{x}_i - \mathbf{x}_j\|^2/\sigma^2)$, where σ
 244 is the kernel width. For the graph regularization term we use a fully connected affinity graph with the
 245 Gaussian kernel weighting on the edges. To choose the parameter σ we perform a simple grid search for
 246 the 40 values of σ in the range of $[0.1, 4]$ with the step size $\Delta\sigma = 0.1$ for data sets Dermatology, Glass,
 247 Soybean and Zoo. For the AT&T face database we perform the grid search in the range $\sigma = [1000, 10000]$
 248 with the step size $\Delta\sigma = 250$. For the Vehicle data set we perform the grid search in the range $\sigma = [10, 100]$
 249 with the step size $\Delta\sigma = 10$. At the boundary values of the σ intervals the clustering accuracy saturates.
 250 For small values of σ the similarity of the data points with large distance $\|\mathbf{x}_i - \mathbf{x}_j\|$ goes to zero as
 251 $\exp(-\|\mathbf{x}_i - \mathbf{x}_j\|^2/\sigma^2) \rightarrow 0$ when $\|\mathbf{x}_i - \mathbf{x}_j\|^2/\sigma^2$ is large. Therefore, for small distances, the affinity graph
 252 captures the local Euclidean distance and gives a good representation of the manifold structure. For
 253 KNSC-Ncut algorithm we used the same grid search to obtain a degree matrix $\mathbf{D}^{-1/2}$.

254 For each data set, we measure the average clustering accuracy out of 256 independent runs. We
 255 perform a hold-out validation for the parameter σ , as shown in the Table 4. The hold-out validation
 256 consists of randomly splitting each data set into two equally sized parts with the equally distributed
 257 cluster membership. The grid search optimization is performed on the first half of the data set, while
 258 the second half is used as a hold-out validation where optimized parameters are used. The results of the
 259 hold-out validation show robust average clustering accuracy for all three algorithms on all six data sets.

260 The sensitivity analysis of the algorithms is performed for the three trade-off parameters α , μ and
 261 λ , plotted in in Fig. 6 and 7. The ratio of the parameters μ and α is fixed to a constant value in
 262 all experiments. The near-orthogonality of the clustering indicator matrix $\mathbf{H}(\mathbf{Z})$ is preserved during
 263 the multiplicative updates, as shown in Fig. 6 and 7. The near-orthogonality of columns is important
 264 for data clustering interpretation. An orthogonal clustering matrix has an interpretation that each row
 265 of $\mathbf{H}(\mathbf{Z})$ can have only one nonzero element, which implies that each data object belongs only to 1
 266 cluster. We plot the average orthogonality over 256 runs of the clustering matrix \mathbf{H} (KNSC-Rcut) for

267 a wide range of values of the parameter μ and fixed α . The average orthogonality per run is defined
 268 as $\sum_{i,i=1}^k (\mathbf{H}\mathbf{H}^T)_{i,i} / \sum_{i \neq j} (\mathbf{H}\mathbf{H}^T)_{i,j}$. For a wide range of values of the ratio μ/α the orthogonality is
 269 preserved during the updates. In Fig. 6 we plot the corresponding average clustering accuracy for
 270 KNSC-Rcut. When μ becomes a few order of magnitude larger compared to the reconstruction error
 271 term, the objective function effectively becomes the optimization of the orthogonality term. At that
 272 point the reconstruction error term loses its significance and the average clustering accuracy starts to
 273 drop. In Fig. 6 we plot the clustering accuracy in a wide range of values of the parameter μ . The graph
 274 regularization λ is fixed to a constant value $\lambda = \alpha$ for simplicity. The average orthogonality is plotted
 275 for different values of λ and μ parameters in Fig. 6 and 7. The clustering accuracy is robust for a wide
 276 range of λ , $\lambda = [10^{-4} - 10^2]$, and μ , $\mu = [10^0 - 10^7]$ throughout the experiments on all six data sets.

277 4. Conclusion

278 In this paper we study subspace clustering from nonlinear orthogonal non-negative matrix factoriza-
 279 tion perspective. We have constructed a nonlinear orthogonal NMF algorithm and derived three novel
 280 clustering algorithms. We have formally shown that the Rcut spectral clustering is equivalent to the
 281 nonlinear orthonormal NMF. The equivalence with the Ncut spectral clustering is obtained by introduc-
 282 ing an additional scaling matrix into the nonlinear factorization. Based on this equivalence, we have
 283 proposed two kernel-based non-negative spectral clustering methods, KNSC-Ncut and KNSC-Rcut. By
 284 incorporating the graph regularization term into the nonlinear NMF framework we have formulated a
 285 kernel-based graph-regularized orthogonal non-negative matrix factorization (KOGNMF). To solve the
 286 subspace clustering we have derived general kernel-based orthogonal multiplicative updates with com-
 287 plexity $\mathcal{O}(kn^2)$. The monotonic convergence of all three algorithms is proven using an auxiliary function
 288 analogous to that used for proving convergence of the Expectation-Maximization algorithm. Experimental
 289 results show the effectiveness of our methods compared to state-of-the-art recently proposed NMF-based
 290 clustering methods.

291 Acknowledgment

292 The authors would like to thank to Mario Lucic and Maria Brbic for proofreading the article. The
 293 work of DT is funded by the by the Croatian Science Foundation with the project No. I-1701-2014
 294 "Machine learning algorithms for insightful analysis of complex data structures". The work of IK is
 295 funded by Croatian science foundation with the project IP-2016-06-5235 "Structured Decompositions
 296 of Empirical Data for Computationally-Assisted Diagnoses of Disease" and was in part supported by
 297 European Regional Development Fund under the grant KK.01.1.1.01.0009 (DATACROSS). The work of
 298 NAF is funded by the EU Horizon 2020 SoBigData project under grant agreement No. 654024.

299 Appendix A

Proof of Theorem 1. The factorization $\Phi(\mathbf{X})\mathbf{D}^{-1/2} = \mathbf{W}\mathbf{Z}$ can be solved by the following optimization problem

$$\min_{\mathbf{Z}, \mathbf{W}} \|\Phi(\mathbf{X})\mathbf{D}^{-1/2} - \mathbf{W}\mathbf{Z}\|_F^2 \quad s.t. \quad \mathbf{Z}\mathbf{Z}^\top = \mathbf{I}, \quad (46)$$

where $\mathbf{Z}\mathbf{Z}^\top = \mathbf{I}$ is the orthogonality constraint which can be included in the optimization implicitly or explicitly via Lagrange multipliers. Then objective function can be reformulated as $J(\mathbf{Z}, \mathbf{W})$

$$\frac{1}{2} \text{Tr} \left((\Phi(\mathbf{X})\mathbf{D}^{-1/2} - \mathbf{W}\mathbf{Z})^\top (\Phi(\mathbf{X})\mathbf{D}^{-1/2} - \mathbf{W}\mathbf{Z}) \right) \quad (47)$$

$$= \frac{1}{2} \text{Tr} \left((\mathbf{D}^{-1/2}\Phi^\top(\mathbf{X}) - \mathbf{Z}^\top\mathbf{W}^\top) (\Phi(\mathbf{X})\mathbf{D}^{-1/2} - \mathbf{W}\mathbf{Z}) \right) \quad (48)$$

$$= \frac{1}{2} \text{Tr} \left(\Phi(\mathbf{X})\mathbf{D}^{-1}\Phi(\mathbf{X})^\top - 2\mathbf{W}\mathbf{Z}\mathbf{D}^{-1/2}\Phi(\mathbf{X})^\top + \mathbf{W}\mathbf{W}^\top \right). \quad (49)$$

300 The constraint $\mathbf{Z}\mathbf{Z}^\top = \mathbf{I}$ is used in the last equality. Calculating the partial derivative of $J(\mathbf{Z}, \mathbf{W})$ with
301 respect to \mathbf{W} and letting it be equal to 0, it follows

$$\frac{\partial J(\mathbf{Z}, \mathbf{W})}{\partial \mathbf{W}} = -\Phi(\mathbf{X})\mathbf{D}^{-1/2}\mathbf{Z}^\top + \mathbf{W} = 0. \quad (50)$$

From here, we have

$$\mathbf{W} = \Phi(\mathbf{X})\mathbf{D}^{-1/2}\mathbf{Z}^\top \quad (51)$$

302 Substituting (51) back into (49), we obtain $J(\mathbf{Z}, \mathbf{W}) =$

$$\frac{1}{2} \text{Tr} \left(\Phi(\mathbf{X})\mathbf{D}^{-1}\Phi(\mathbf{X})^\top - 2\Phi(\mathbf{X})\mathbf{D}^{-1/2}\mathbf{Z}^\top\mathbf{Z}\mathbf{D}^{-1/2}\Phi(\mathbf{X})^\top \right). \quad (52)$$

Since $\Phi(\mathbf{X})\mathbf{D}^{-1}\Phi(\mathbf{X})^\top$ is not dependent on \mathbf{Z} and \mathbf{W} , the minimization problem is equivalent to

$$\max_{\mathbf{Z}, \mathbf{W}} \text{Tr} \left(\mathbf{Z}\mathbf{D}^{-1/2}\Phi(\mathbf{X})^\top\Phi(\mathbf{X})\mathbf{D}^{-1/2}\mathbf{Z}^\top \right) \quad s.t. \quad \mathbf{Z}\mathbf{Z}^\top = \mathbf{I}. \quad (53)$$

For $\mathbf{A} = \Phi^\top(\mathbf{X})\Phi(\mathbf{X})$ the objective function (53) is

$$\max_{\mathbf{Z}} \text{Tr} \left(\mathbf{Z}\mathbf{D}^{-1/2}\mathbf{A}\mathbf{D}^{-1/2}\mathbf{Z}^\top \right) \quad s.t. \quad \mathbf{Z}\mathbf{Z}^\top = \mathbf{I}. \quad (54)$$

Note, that the objective function for Ncut spectral clustering

$$\min_{\mathbf{Z}} \text{Tr} \left(\mathbf{Z}\mathbf{L}_{sym}\mathbf{Z}^\top \right) \quad s.t. \quad \mathbf{Z}\mathbf{Z}^\top = \mathbf{I}. \quad (55)$$

can easily be transformed to (53).

$$\min_{\mathbf{Z}, \mathbf{Z}\mathbf{Z}^\top = \mathbf{I}} \text{Tr} \left(\mathbf{Z}\mathbf{D}^{-1/2}(\mathbf{D} - \mathbf{A})\mathbf{D}^{-1/2}\mathbf{Z}^\top \right) = \quad (56)$$

$$\min_{\mathbf{Z}, \mathbf{Z}\mathbf{Z}^T = \mathbf{I}} \text{Tr} \left(\mathbf{Z}\mathbf{D}^{-1/2}\mathbf{D}\mathbf{D}^{-1/2}\mathbf{Z}^T - \mathbf{Z}\mathbf{D}^{-1/2}\mathbf{A}\mathbf{D}^{-1/2}\mathbf{Z}^T \right) = \quad (57)$$

and since the term $\mathbf{Z}\mathbf{D}^{-1/2}\mathbf{D}\mathbf{D}^{-1/2}\mathbf{Z}^T = \mathbf{I}$ due to the orthogonality $\mathbf{Z}\mathbf{Z}^T = \mathbf{I}$ this is equal to maximization of the second term.

$$\max_{\mathbf{Z}, \mathbf{Z}\mathbf{Z}^T = \mathbf{I}} \text{Tr} \left(\mathbf{Z}\mathbf{D}^{-1/2}\mathbf{A}\mathbf{D}^{-1/2}\mathbf{Z}^T \right). \quad (58)$$

303 which concludes the proof.

Proof of Theorem 2. For the Rcut spectral clustering we solve the factorization $\Phi(\mathbf{X}) = \mathbf{W}\mathbf{H}$, with constraint $\mathbf{H}\mathbf{H}^T = \mathbf{I}$. The factorization $\Phi(\mathbf{X}) = \mathbf{W}\mathbf{H}$ can be solved by the optimization problem

$$\min_{\mathbf{H}, \mathbf{W}, \mathbf{H}\mathbf{H}^T = \mathbf{I}} \|\Phi(\mathbf{X}) - \mathbf{W}\mathbf{H}\|_F^2, \quad (59)$$

where $\mathbf{H}\mathbf{H}^T = \mathbf{I}$ is the orthogonality constraint which can be included in the optimization implicitly or explicitly. The objective function (59) can be reformulated as

$$J(\mathbf{H}, \mathbf{W}) = \frac{1}{2} \text{Tr} \left((\Phi(\mathbf{X}) - \mathbf{W}\mathbf{H})^T (\Phi(\mathbf{X}) - \mathbf{W}\mathbf{H}) \right) = \quad (60)$$

$$= \frac{1}{2} \text{Tr} \left((\Phi^T(\mathbf{X}) - \mathbf{H}^T\mathbf{W}^T) (\Phi(\mathbf{X}) - \mathbf{W}\mathbf{H}) \right) = \quad (61)$$

$$= \frac{1}{2} \text{Tr} \left(\Phi(\mathbf{X})^T \Phi(\mathbf{X}) - 2\Phi(\mathbf{X})^T \mathbf{W}\mathbf{H} + \mathbf{W}^T \mathbf{W} \right). \quad (62)$$

304 The constraint $\mathbf{H}\mathbf{H}^T = \mathbf{I}$ is used in the last equality. Calculating the partial derivative of $J(\mathbf{H}, \mathbf{W})$ with
305 respect to \mathbf{W} and letting it be equal to 0, it follows

$$\frac{\partial J(\mathbf{H}, \mathbf{W})}{\partial \mathbf{W}} = -\Phi(\mathbf{X})\mathbf{H}^T + \mathbf{W} = 0. \quad (63)$$

From here, we have

$$\mathbf{W} = \Phi(\mathbf{X})\mathbf{H}^T. \quad (64)$$

Substituting (64) back into (62), we obtain

$$J(\mathbf{H}) = \frac{1}{2} \text{Tr} \left(\Phi(\mathbf{X})^T \Phi(\mathbf{X}) - \Phi(\mathbf{X})^T \Phi(\mathbf{X})\mathbf{H}^T \mathbf{H} \right). \quad (65)$$

Since the first term is constant, not dependent on \mathbf{H} and \mathbf{W} , the minimization problem is equivalent to

$$\max_{\mathbf{H}, \mathbf{W}, \mathbf{H}\mathbf{H}^T = \mathbf{I}} \text{Tr} \left(\mathbf{H}\Phi(\mathbf{X})^T \Phi(\mathbf{X})\mathbf{H}^T \right). \quad (66)$$

For $\mathbf{A} = \Phi^T(\mathbf{X})\Phi(\mathbf{X})$ the objective function (66) is the same as objective function (58) for the relaxed Rcut spectral clustering. To see why, we start from the objective function of Rcut and come to the relaxed Rcut optimization function [29]:

$$\min_{\mathbf{H}, \mathbf{H}\mathbf{H}^T = \mathbf{I}} \text{Tr} \left(\mathbf{H}\mathbf{L}\mathbf{H}^T \right) = \min_{\mathbf{H}, \mathbf{H}\mathbf{H}^T = \mathbf{I}} \text{Tr} \left(\mathbf{H}\mathbf{D}\mathbf{H}^T - \mathbf{H}\mathbf{A}\mathbf{H}^T \right). \quad (67)$$

Now, the substitution is made $\mathbf{Q} = \mathbf{H}\mathbf{D}^{1/2}$ which implies $\mathbf{H} = \mathbf{Q}\mathbf{D}^{-1/2}$, $\mathbf{H}\mathbf{H}^\top = \mathbf{Q}\mathbf{D}^{-1}\mathbf{Q}^\top$ and the objective function can be written as:

$$\begin{aligned} & \min_{\mathbf{Q}, \mathbf{Q}\mathbf{D}^{-1}\mathbf{Q}^\top = \mathbf{I}} \text{Tr} \left(\mathbf{Q}\mathbf{D}^{-1/2}\mathbf{D}\mathbf{D}^{-1/2}\mathbf{Q}^\top - \mathbf{Q}\mathbf{D}^{-1/2}\mathbf{A}\mathbf{D}^{-1/2}\mathbf{Q}^\top \right) \\ & = \min_{\mathbf{Q}, \mathbf{Q}\mathbf{D}^{-1}\mathbf{Q}^\top = \mathbf{I}} \text{Tr} \left(\mathbf{Q}\mathbf{Q}^\top - \mathbf{Q}\mathbf{D}^{-1/2}\mathbf{A}\mathbf{D}^{-1/2}\mathbf{Q}^\top \right). \end{aligned} \quad (68)$$

The expression (68) is equivalent to

$$\max_{\mathbf{Q}, \mathbf{Q}\mathbf{D}^{-1}\mathbf{Q}^\top = \mathbf{I}} \text{Tr} \left(\mathbf{Q}\mathbf{D}^{-1/2}\mathbf{A}\mathbf{D}^{-1/2}\mathbf{Q}^\top \right) \quad s.t. \quad \mathbf{Q}\mathbf{Q}^\top = \mathbf{I} \quad (69)$$

Next, we release the orthonormality constraint $\mathbf{Q}\mathbf{Q}^\top = \mathbf{I}$. The relaxation is justified by the fact that the rows of \mathbf{Q} are orthogonal to each other since $\mathbf{Q}\mathbf{D}^{-1}\mathbf{Q}^\top = \mathbf{I}$.

$$\max_{\mathbf{Q}, \mathbf{Q}\mathbf{D}^{-1}\mathbf{Q}^\top = \mathbf{I}} \text{Tr} \left(\mathbf{Q}\mathbf{D}^{-1/2}\mathbf{A}\mathbf{D}^{-1/2}\mathbf{Q}^\top \right) \quad (70)$$

and by substitution $\mathbf{Q} = \mathbf{H}\mathbf{D}^{1/2}$ this becomes:

$$\max_{\mathbf{H}, \mathbf{H}\mathbf{H}^\top = \mathbf{I}} \text{Tr} (\mathbf{H}\mathbf{A}\mathbf{H}) \quad (71)$$

306 which is equal to objective function of (66), which concludes the proof.

307 Appendix B

308 **Proof 3. The convergence analysis of the proposed algorithms.**

309 We now show the algorithm KOGNMF converges to a feasible solution. We use the auxiliary function
310 approach, following [32, 7]. The convergence of KNCS-Ncut and KNCS-Rcut can be proven in a similar
311 way.

312 The objective function of KOGNMF (36) is non-increasing under the alternative iterative updating
313 rules in (37) and (38).

314 **Definition.** $A(h, h')$ is an auxiliary function for $B(h)$ when the following conditions are satisfied:

$$A(h, h') \geq B(h), \quad A(h, h) = B(h). \quad (72)$$

315 The auxiliary function is useful because of the following lemma:

316 **Lemma 1.** If A is an auxiliary function of B , then B is non-increasing under the updating formula

$$h^{(t+1)} = \arg \min_h A(h, h^{(t)}) \quad (73)$$

317 the function B is non-increasing.

318 **Proof.** $B(h^{(t+1)}) \leq A(h^{(t+1)}, h^{(t)}) \leq A(h^{(t)}, h^{(t)}) = B(h^{(t)})$.

319 We now rewrite the objective function \mathcal{L} of KOGNMF in Eq. (36) as follows

$$\begin{aligned} \mathcal{L} &= \alpha \|\Phi(\mathbf{X}) - \Phi(\mathbf{X})\mathbf{F}\mathbf{H}\|_F^2 + \lambda \text{Tr}(\mathbf{H}\mathbf{L}\mathbf{H}^\top) + \mu \|\mathbf{H}\mathbf{H}^\top - \mathbf{I}_k\|_F^2 \\ &= \alpha \sum_{i=1}^D \sum_{j=1}^n \left(\Phi(x)_{ij} - \sum_{l=1}^k w_{il} h_{lj} \right)^2 + \lambda \sum_{m=1}^k \sum_{j=1}^n \sum_{l=1}^n h_{mj} L_{jl} h_{lm} + \mu \sum_{i=1}^D \sum_{j=1}^n \left(\sum_{l=1}^n h_{ik} h_{kj} - \delta_{ij} \right)^2 \end{aligned} \quad (74)$$

320 Considering any element h_{ab} in \mathbf{H} , we use B_{ab} to denote the part of \mathcal{L} relevant to h_{ab} . Then it follows

$$\dot{B}_{ab} \equiv \left(\frac{\partial \mathcal{L}}{\partial \mathbf{H}} \right)_{ab} = \left(2\alpha \mathbf{F}^\top \mathbf{K} \mathbf{F} \mathbf{H} - 2\alpha \mathbf{F}^\top \mathbf{K} + 2\lambda \mathbf{H} \mathbf{L} + 4\mu \mathbf{H} (\mathbf{H}^\top \mathbf{H} - \mathbf{I}) \right)_{ab} \quad (75)$$

321 Since multiplicative update rules are element-wise, we have to show that each B_{ab} is non-increasing
322 under the update step given in Eq. (37).

Lemma 2. Function

$$A(h, h_{ab}^{(t)}) = B(h_{ab}^{(t)}) + \dot{B}_{ab}(h_{ab}^{(t)})(h - h_{ab}^{(t)}) + \frac{(2\alpha \mathbf{F}^\top \mathbf{K} \mathbf{F} \mathbf{H} + 2\lambda \mathbf{H} \mathbf{D})_{ab}}{h_{ab}^{(t)}} (h - h_{ab}^{(t)})^2. \quad (76)$$

323 is an auxiliary function for B_{ab} , when $\mu = 0$.

Proof. By the above equation, we have $A(h, h) = B_{ab}(h)$, so we only need to show that $A(h, h_{ab}^{(t)}) \geq B_{ab}(h)$. To this end, we compare the auxiliary function given in Eq. (76) with the Taylor expansion of $B_{ab}(h)$.

$$\ddot{B}_{ab} \equiv \left(\frac{\partial^2 \mathcal{L}}{\partial \mathbf{H}^2} \right)_{ab} = \left(2\alpha \mathbf{F}^\top \mathbf{K} \mathbf{F} + 2\lambda \mathbf{L} \right)_{ab} \quad (77)$$

$$B_{ab}(h) = B_{ab}(h_{ab}^{(t)}) + \dot{B}_{ab}(h - h_{ab}^{(t)}) + [\alpha \mathbf{F}^\top \mathbf{K} \mathbf{F} + \lambda \mathbf{L}]_{ab} (h - h_{ab}^{(t)})^2 \quad (78)$$

324 to find that $A(h, h_{ab}^{(t)}) \geq B_{ab}(h)$ is equivalent to

$$\frac{\alpha (\mathbf{F}^\top \mathbf{K} \mathbf{F} \mathbf{H})_{ab} + \lambda (\mathbf{H} \mathbf{D})_{ab}}{h_{ab}^{(t)}} \geq (\alpha \mathbf{F}^\top \mathbf{K} \mathbf{F} + \lambda \mathbf{L})_{ab} \quad (79)$$

$$(\mathbf{F}^\top \mathbf{K} \mathbf{F} \mathbf{H})_{ab} = \sum_{l=1}^k (\mathbf{F}^\top \mathbf{K} \mathbf{F})_{al} h_{lb}^{(t)} \geq (\mathbf{F}^\top \mathbf{K} \mathbf{F})_{aa} h_{ab}^{(t)} \quad (80)$$

$$(\mathbf{H} \mathbf{D})_{ab} = \sum_{l=1}^n h_{al}^{(t)} \mathbf{D}_{lb} \geq h_{ab}^{(t)} \mathbf{D}_{bb} \geq h_{ab}^{(t)} (\mathbf{D} - \mathbf{A})_{bb} \quad (81)$$

325 In summary, we have the following inequality

$$\frac{(\alpha \mathbf{F}^\top \mathbf{K} \mathbf{F} \mathbf{H} + \lambda \mathbf{H} \mathbf{D})_{ab}}{h_{ab}^{(t)}} \geq \frac{1}{2} \ddot{B}_{ab} \quad (82)$$

326 Then the inequality $A(h, h_{ab}^{(t)}) \geq B_{ab}(h)$ is satisfied, and the Lemma is proven.

327 From Lemma 2, we know that $A(h, h_{ab}^t)$ is an auxiliary function of $B_{ab}(h_{ab})$. We can now demonstrate
328 the convergence of the update rules given in Eqs. (37).

$$h^{t+1} = \arg \min_h A(h, h^{(t)}) \quad (83)$$

$$h_{ab}^{t+1} = h_{ab}^t \frac{(\alpha \mathbf{F}^\top \mathbf{K} + \lambda \mathbf{H} \mathbf{A})_{ab}}{(\alpha \mathbf{F}^\top \mathbf{K} \mathbf{F} \mathbf{H} + \lambda \mathbf{H} \mathbf{D})_{ab}} \quad (84)$$

329 So the updating rule for H is as follows:

$$H_{ab} \leftarrow H_{ab} \frac{(\alpha \mathbf{F}^\top \mathbf{K} + \lambda \mathbf{H} \mathbf{A})_{ab}}{(\alpha \mathbf{F}^\top \mathbf{K} \mathbf{F} \mathbf{H} + \lambda \mathbf{H} \mathbf{D})_{ab}} \quad (85)$$

330 Similarly, for $\mu > 0$, we use the following auxiliary function $A(h, h_{ab}^t) =$

$$A(h, h_{ab}^t) = B(h_{ab}^t) + \dot{B}_{ab}(h_{ab}^t)(h - h_{ab}^t) + \frac{\alpha(\mathbf{F}^\top \mathbf{K} \mathbf{F} \mathbf{H})_{ab} + \lambda(\mathbf{H} \mathbf{D})_{ab} + \mu(\mathbf{H} \mathbf{H}^\top \mathbf{H})_{ab}}{h_{ab}^t} (h - h_{ab}^t)^2. \quad (86)$$

and by using this:

$$(\mathbf{H} \mathbf{H}^\top \mathbf{H})_{ab} = \sum_{l=1}^n h_{al}^t (\mathbf{H}^\top \mathbf{H})_{lb} \geq h_{ab}^t (\mathbf{H}^\top \mathbf{H})_{bb} \quad (87)$$

we obtain the following inequality

$$\frac{\alpha(\mathbf{F}^\top \mathbf{K} \mathbf{F} \mathbf{H})_{ab} + \lambda(\mathbf{H} \mathbf{D})_{ab} + \mu(\mathbf{H} \mathbf{H}^\top \mathbf{H})_{ab}}{h_{ab}^t} \geq (\alpha \mathbf{F}^\top \mathbf{K} \mathbf{F} + \mu \mathbf{H}^\top \mathbf{H} + \lambda \mathbf{L})_{ab} \quad (88)$$

which is used to prove that (86) is an auxiliary function of (74). Finally, we get the update rule

$$H_{ab} \leftarrow H_{ab} \frac{(\alpha \mathbf{F}^\top \mathbf{K} + 2\mu \mathbf{H} + \lambda \mathbf{H} \mathbf{A})_{ab}}{(\alpha \mathbf{F}^\top \mathbf{K} \mathbf{F} \mathbf{H} + 2\mu \mathbf{H} \mathbf{H}^\top \mathbf{H} + \lambda \mathbf{H} \mathbf{D})_{ab}}. \quad (89)$$

The proof of the convergence for the \mathbf{F} update rule (38) can be derived by following proposition 8 from [7]. The auxiliary function for our objective function $\mathcal{L}(\mathbf{F})$ (39) as a function of \mathbf{F} is:

$$A(\mathbf{F}, \mathbf{F}') = - \sum_{i,k} 2(\mathbf{K} \mathbf{H}^\top)_{i,k} \mathbf{F}'_{i,k} (1 + \log \frac{\mathbf{F}_{i,k}}{\mathbf{F}'_{i,k}}) + \sum_{i,k} \frac{(\mathbf{K} \mathbf{F}' \mathbf{H} \mathbf{H}^\top)_{i,k} (\mathbf{F}_{i,k})^2}{\mathbf{F}'_{i,k}}, \quad (90)$$

The proof that this is an auxiliary function of $\mathcal{L}(\mathbf{F})$ (39) is given in [7], with the change in notation $\mathbf{F} = \mathbf{W}$, $\mathbf{H} = \mathbf{G}^\top$ and $\Phi(\mathbf{X}) = \mathbf{X}$.

This auxiliary function is a convex function of F and it's global minimum can be derived with the following update rule:

$$F_{ab} \leftarrow F_{ab} \frac{(\mathbf{K} \mathbf{H}^\top)_{ab}}{(\mathbf{K} \mathbf{F} \mathbf{H} \mathbf{H}^\top)_{ab}}. \quad (91)$$

331 **References**

- 332 [1] H. S. Seung, D. D. Lee, Learning the parts of objects by non-negative matrix factorization, *Nature*
333 401 (6755) (1999) 788–791. doi:10.1038/44565.
334 URL <http://dx.doi.org/10.1038/44565>
- 335 [2] C. Ding, T. Li, M. I. Jordan, Nonnegative matrix factorization for combinatorial optimization:
336 Spectral clustering, graph matching, and clique finding, in: 2008 Eighth IEEE International Con-
337 ference on Data Mining, Institute of Electrical and Electronics Engineers (IEEE), 2008. doi:
338 10.1109/icdm.2008.130.
339 URL <http://dx.doi.org/10.1109/icdm.2008.130>
- 340 [3] S. Yang, Z. Yi, M. Ye, X. He, Convergence analysis of graph regularized non-negative matrix
341 factorization, *IEEE Transactions on Knowledge and Data Engineering* 26 (9) (2014) 2151–2165.
342 doi:10.1109/tkde.2013.98.
343 URL <http://dx.doi.org/10.1109/tkde.2013.98>
- 344 [4] D. Cai, X. He, J. Han, T. S. Huang, Graph regularized nonnegative matrix factorization for data
345 representation, *IEEE Transactions on Pattern Analysis and Machine Intelligence* 33 (8) (2011) 1548–
346 1560. doi:10.1109/tpami.2010.231.
347 URL <http://dx.doi.org/10.1109/tpami.2010.231>
- 348 [5] S. Choi, Algorithms for orthogonal nonnegative matrix factorization, in: 2008 IEEE International
349 Joint Conference on Neural Networks (IEEE World Congress on Computational Intelligence), Insti-
350 tute of Electrical and Electronics Engineers (IEEE), 2008. doi:10.1109/ijcnn.2008.4634046.
351 URL <http://dx.doi.org/10.1109/ijcnn.2008.4634046>
- 352 [6] C. Ding, T. Li, W. Peng, H. Park, Orthogonal nonnegative matrix t-factorizations for clustering, in:
353 Proceedings of the 12th ACM SIGKDD international conference on Knowledge discovery and data
354 mining - KDD 06, Association for Computing Machinery (ACM), 2006. doi:10.1145/1150402.
355 1150420.
356 URL <http://dx.doi.org/10.1145/1150402.1150420>
- 357 [7] C. Ding, T. Li, M. Jordan, Convex and semi-nonnegative matrix factorizations, *IEEE Transactions*
358 *on Pattern Analysis and Machine Intelligence* 32 (1) (2010) 45–55. doi:10.1109/tpami.2008.277.
359 URL <http://dx.doi.org/10.1109/tpami.2008.277>
- 360 [8] F. Pompili, N. Gillis, P.-A. Absil, F. Glineur, Two algorithms for orthogonal nonnegative matrix
361 factorization with application to clustering, *Neurocomputing* 141 (2014) 15–25. doi:10.1016/j.
362 neucom.2014.02.018.
363 URL <http://dx.doi.org/10.1016/j.neucom.2014.02.018>

- 364 [9] H. Lee, A. Cichocki, S. Choi, Kernel nonnegative matrix factorization for spectral EEG feature
365 extraction, *Neurocomputing* 72 (13-15) (2009) 3182–3190. doi:10.1016/j.neucom.2009.03.005.
366 URL <http://dx.doi.org/10.1016/j.neucom.2009.03.005>
- 367 [10] B. Pan, J. Lai, W.-S. Chen, Nonlinear nonnegative matrix factorization based on mercer kernel
368 construction, *Pattern Recognition* 44 (10–11) (2011) 2800 – 2810, semi-Supervised Learning for
369 Visual Content Analysis and Understanding.
- 370 [11] E. E., V. R., Sparse subspace clustering: Algorithm, theory, and applications, *IEEE Trans. Patt.*
371 *Anal. Mach. Intel.* 35 (1) (2013) 2765–2781.
- 372 [12] L. G., Z. Lin, Y. S., S. J., Y. Y., M. Y., Robust recovery of subspace structures by low-rank
373 representation, *IEEE Trans. Patt. Anal. Mach. Intel.* 35 (1) (2013) 171–184.
- 374 [13] L. C.-G., V. R., A structured sparse plus structured low-rank framework for subspace clustering and
375 completion, *IEEE Trans. Sig. Proc.* 64 (24) (2016) 6557–6570.
- 376 [14] L. C.-G., V. R., Diversity-induced multi-view subspace clustering, *IEEE Trans. Sig. Proc.* 64 (24)
377 (2016) 6557–6570.
- 378 [15] M. Brbic, I. Kopriva, Multi-view low-rank sparse subspace clustering, *Pattern Recognition* 73 (2018)
379 247–258.
- 380 [16] L. W. Liu, G. C., H. J., Multi-view clustering via joint nonnegative matrix factorisation, *Proc. SIAM*
381 *Int. Conf. Data Mining (SDM'13)* 73 (2013) 252–260.
- 382 [17] D.-S. Pham, O. Arandjelovic, S. Venkatesh, Achieving stable subspace clustering by post-processing
383 generic clustering results, *IEEE International Joint Conference on Neural Networks (IJCNN)*.
- 384 [18] M. Filippone, F. Camastra, F. Masulli, S. Rovetta, A survey of kernel and spectral methods for
385 clustering, *Pattern Recognition* 41 (1) (2008) 176–190. doi:10.1016/j.patcog.2007.05.018.
386 URL <http://dx.doi.org/10.1016/j.patcog.2007.05.018>
- 387 [19] A. Y. Ng, M. I. Jordan, Y. Weiss, et al., On spectral clustering: Analysis and an algorithm, *Advances*
388 *in neural information processing systems* 2 (2002) 849–856.
- 389 [20] Y. Liu, X. Li, C. Liu, H. Liu, Structure-constrained low-rank and partial sparse representation
390 with sample selection for image classification, *Pattern Recognition* 59 (2016) 5–13. doi:10.1016/
391 j.patcog.2016.01.026.
392 URL <http://dx.doi.org/10.1016/j.patcog.2016.01.026>

- 393 [21] S. White, P. Smyth, A spectral clustering approach to finding communities in graphs, in: Proceed-
394 ings of the 2005 SIAM International Conference on Data Mining, Society for Industrial & Applied
395 Mathematics (SIAM), 2005, pp. 274–285. doi:10.1137/1.9781611972757.25.
396 URL <http://dx.doi.org/10.1137/1.9781611972757.25>
- 397 [22] F. R. Bach, M. I. Jordan, Spectral clustering for speech separation, in: Automatic Speech and
398 Speaker Recognition, Wiley-Blackwell, pp. 221–250. doi:10.1002/9780470742044.ch13.
399 URL <http://dx.doi.org/10.1002/9780470742044.ch13>
- 400 [23] H. Jia, S. Ding, H. Ma, W. Xing, Spectral clustering with neighborhood attribute reduction based
401 on information entropy, JCP 9 (6). doi:10.4304/jcp.9.6.1316-1324.
402 URL <http://dx.doi.org/10.4304/jcp.9.6.1316-1324>
- 403 [24] H. Jia, S. Ding, X. Xu, R. Nie, The latest research progress on spectral clustering, Neural Computing
404 and Applications 24 (7-8) (2013) 1477–1486. doi:10.1007/s00521-013-1439-2.
405 URL <http://dx.doi.org/10.1007/s00521-013-1439-2>
- 406 [25] J. Lurie, Review of spectral graph theory, ACM SIGACT News 30 (2) (1999) 14. doi:10.1145/
407 568547.568553.
408 URL <http://dx.doi.org/10.1145/568547.568553>
- 409 [26] U. von Luxburg, A tutorial on spectral clustering, Statistics and Computing 17 (4) (2007) 395–416.
410 doi:10.1007/s11222-007-9033-z.
411 URL <http://dx.doi.org/10.1007/s11222-007-9033-z>
- 412 [27] W. Ju, D. Xiang, B. Zhang, L. Wang, I. Kopriva, X. Chen, Random walk and graph cut for co-
413 segmentation of lung tumor on pet-ct images, IEEE TRANSACTIONS ON IMAGE PROCESSING
414 25 (3) (2016) 1192–1192.
- 415 [28] R. Langone, R. Mall, C. Alzate, J. A. K. Suykens, Kernel spectral clustering and applications,
416 in: Unsupervised Learning Algorithms, Springer Science Business Media, 2016, pp. 135–161. doi:
417 10.1007/978-3-319-24211-8_6.
418 URL http://dx.doi.org/10.1007/978-3-319-24211-8_6
- 419 [29] H. Lu, Z. Fu, X. Shu, Non-negative and sparse spectral clustering, Pattern Recognition 47 (1) (2014)
420 418–426. doi:10.1016/j.patcog.2013.07.003.
421 URL <http://dx.doi.org/10.1016/j.patcog.2013.07.003>
- 422 [30] C. Ding, X. He, H. D. Simon, On the equivalence of nonnegative matrix factorization and spectral
423 clustering, in: Proceedings of the 2005 SIAM International Conference on Data Mining, Society for

- 424 Industrial & Applied Mathematics (SIAM), 2005, pp. 606–610. doi:10.1137/1.9781611972757.70.
425 URL <http://dx.doi.org/10.1137/1.9781611972757.70>
- 426 [31] D. Luo, C. Ding, H. Huang, T. Li, Non-negative laplacian embedding, in: 2009 Ninth IEEE Interna-
427 tional Conference on Data Mining, Institute of Electrical and Electronics Engineers (IEEE), 2009.
428 doi:10.1109/icdm.2009.74.
429 URL <http://dx.doi.org/10.1109/icdm.2009.74>
- 430 [32] R. Shang, Z. Zhang, L. Jiao, W. Wang, S. Yang, Global discriminative-based nonnegative spectral
431 clustering, Pattern Recognition 55 (2016) 172–182. doi:10.1016/j.patcog.2016.01.035.
432 URL <http://dx.doi.org/10.1016/j.patcog.2016.01.035>
- 433 [33] Y. Bengio, O. Delalleau, N. L. Roux, J.-F. Paiement, P. Vincent, M. Ouimet, Learning eigenfunctions
434 links spectral embedding and kernel PCA, Neural Computation 16 (10) (2004) 2197–2219. doi:
435 10.1162/0899766041732396.
436 URL <http://dx.doi.org/10.1162/0899766041732396>
- 437 [34] C. Alzate, J. Suykens, A weighted kernel PCA formulation with out-of-sample extensions for spectral
438 clustering methods, in: The 2006 IEEE International Joint Conference on Neural Network Proceed-
439 ings, Institute of Electrical and Electronics Engineers (IEEE), 2006. doi:10.1109/ijcnn.2006.
440 246671.
441 URL <https://doi.org/10.1109/ijcnn.2006.246671>
- 442 [35] P. Li, J. Bu, Y. Yang, R. Ji, C. Chen, D. Cai, Discriminative orthogonal nonnegative matrix fac-
443 torization with flexibility for data representation, Expert Systems with Applications 41 (4) (2014)
444 1283–1293. doi:10.1016/j.eswa.2013.08.026.
445 URL <http://dx.doi.org/10.1016/j.eswa.2013.08.026>
- 446 [36] D. D. Lee, H. S. Seung, Algorithms for non-negative matrix factorization, in: In NIPS, MIT Press,
447 2000, pp. 556–562.
- 448 [37] X. Peng, H. Tang, L. Zhang, Z. Yi, S. Xiao, A unified framework for representation-based subspace
449 clustering of out-of-sample and large-scale data, IEEE Transactions on Neural Networks and Learning
450 Systems (2015) 1–14doi:10.1109/tnnls.2015.2490080.
451 URL <http://dx.doi.org/10.1109/tnnls.2015.2490080>
- 452 [38] C. Hou, F. Nie, D. Yi, D. Tao, Discriminative embedded clustering: A framework for grouping
453 high-dimensional data, IEEE Transactions on Neural Networks and Learning Systems 26 (6) (2015)
454 1287–1299. doi:10.1109/tnnls.2014.2337335.
455 URL <https://doi.org/10.1109/tnnls.2014.2337335>

- 456 [39] Y. Ma, H. Derksen, W. Hong, J. Wright, Segmentation of multivariate mixed data via lossy data
457 coding and compression, *IEEE Transactions on Pattern Analysis and Machine Intelligence* 29 (9)
458 (2007) 1546–1562. doi:10.1109/tpami.2007.1085.
459 URL <https://doi.org/10.1109/2Ftpami.2007.1085>
- 460 [40] S. R. Rao, R. Tron, R. Vidal, Y. Ma, Motion segmentation via robust subspace separation in the
461 presence of outlying, incomplete, or corrupted trajectories, in: 2008 IEEE Conference on Computer
462 Vision and Pattern Recognition, Institute of Electrical and Electronics Engineers (IEEE), 2008.
463 doi:10.1109/cvpr.2008.4587437.
464 URL <https://doi.org/10.1109/2Fcvpr.2008.4587437>
- 465 [41] M. Belkin, P. Niyogi, Laplacian eigenmaps for dimensionality reduction and data representation,
466 *Neural Computation* 15 (6) (2003) 1373–1396. doi:10.1162/089976603321780317.
467 URL <http://dx.doi.org/10.1162/089976603321780317>
- 468 [42] J. Shi, J. Malik, Normalized cuts and image segmentation, in: Proceedings of IEEE Computer Society
469 Conference on Computer Vision and Pattern Recognition, Institute of Electrical and Electronics
470 Engineers (IEEE). doi:10.1109/cvpr.1997.609407.
471 URL <http://dx.doi.org/10.1109/cvpr.1997.609407>
- 472 [43] C.-K. Cheng, Y.-C. Wei, An improved two-way partitioning algorithm with stable performance
473 (VLSI), *IEEE Transactions on Computer-Aided Design of Integrated Circuits and Systems* 10 (12)
474 (1991) 1502–1511. doi:10.1109/43.103500.
475 URL <http://dx.doi.org/10.1109/43.103500>
- 476 [44] P. K. Chan, M. D. F. Schlag, J. Y. Zien, Spectral k -way ratio-cut partitioning and clustering, in:
477 Proceedings of the 30th international on Design automation conference - DAC 93, Association for
478 Computing Machinery (ACM), 1993. doi:10.1145/157485.165117.
479 URL <http://dx.doi.org/10.1145/157485.165117>
- 480 [45] N. Gillis, S. A. Vavasis, Fast and robust recursive algorithms for separable nonnegative matrix fac-
481 torization, *IEEE Transactions on Pattern Analysis and Machine Intelligence* 36 (4) (2014) 698–714.
482 doi:10.1109/tpami.2013.226.
483 URL <http://dx.doi.org/10.1109/tpami.2013.226>
- 484 [46] A. N. Langville, C. D. Meyer, R. Albright, Initializations for the nonnegative matrix factorization
485 (KDD 2006).
- 486 [47] B. Scholkopf, A. J. Smola, Learning with Kernels: Support Vector Machines, Regularization, Opti-
487 mization, and Beyond, MIT Press, Cambridge, MA, USA, 2001.

- 488 [48] T.-M. Huang, V. Kecman, I. Kopriva, Kernel Based Algorithms for Mining Huge Data Sets: Su-
489 pervised, Semi-supervised, and Unsupervised Learning (Studies in Computational Intelligence),
490 Springer-Verlag New York, Inc., Secaucus, NJ, USA, 2006.
- 491 [49] D. Cai, X. Wang, X. He, Probabilistic dyadic data analysis with local and global consistency, in:
492 Proceedings of the 26th Annual International Conference on Machine Learning - ICML 09, Associ-
493 ation for Computing Machinery (ACM), 2009. doi:10.1145/1553374.1553388.
494 URL <http://dx.doi.org/10.1145/1553374.1553388>
- 495 [50] X. Niyogi, Locality preserving projections, in: Neural information processing systems, Vol. 16, MIT,
496 2004, p. 153.
- 497 [51] J. J.-Y. Wang, J. Z. Huang, Y. Sun, X. Gao, Feature selection and multi-kernel learning for adaptive
498 graph regularized nonnegative matrix factorization, Expert Systems with Applications 42 (3) (2015)
499 1278–1286. doi:10.1016/j.eswa.2014.09.008.
500 URL <http://dx.doi.org/10.1016/j.eswa.2014.09.008>
- 501 [52] A. Frank, A. Asuncion, Uci machine learning repository, <http://archive.ics.uci.edu/ml/>.
- 502 [53] F. Samaria, A. Harter, Parameterisation of a stochastic model for human face identification, in:
503 Proceedings of 1994 IEEE Workshop on Applications of Computer Vision, Institute of Electrical and
504 Electronics Engineers (IEEE). doi:10.1109/acv.1994.341300.
505 URL <http://dx.doi.org/10.1109/acv.1994.341300>

Biographies of authors



2015

2010 2015

2015



2015

2016



K

1 8

2001 2005

2006